

# GLUONIC STRUCTURE OF THE PION USING TAGGED DIS AT SMALL-X

QCD with Electron Ion Collider(QEIC)-II  
Indian Institute of Technology Delhi (Dec 18-20, 2022)

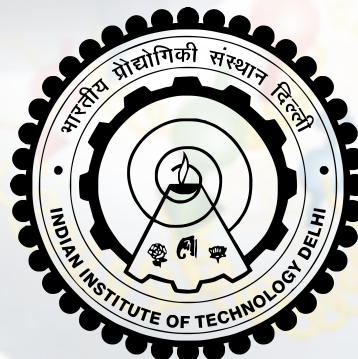
Arjun Kumar (IIT Delhi)

A.Kumar arXiv: 2208.14200

A.Kumar, T.Toll PRD 105 (2022) 114045



विज्ञान एवं प्रौद्योगिकी विभाग  
DEPARTMENT OF  
**SCIENCE & TECHNOLOGY**





# OUTLINE

---

## ➤ Introduction to Tagged-DIS (TDIS)

## ➤ Inclusive $\gamma^* \pi^*$ cross section in leading neutron events

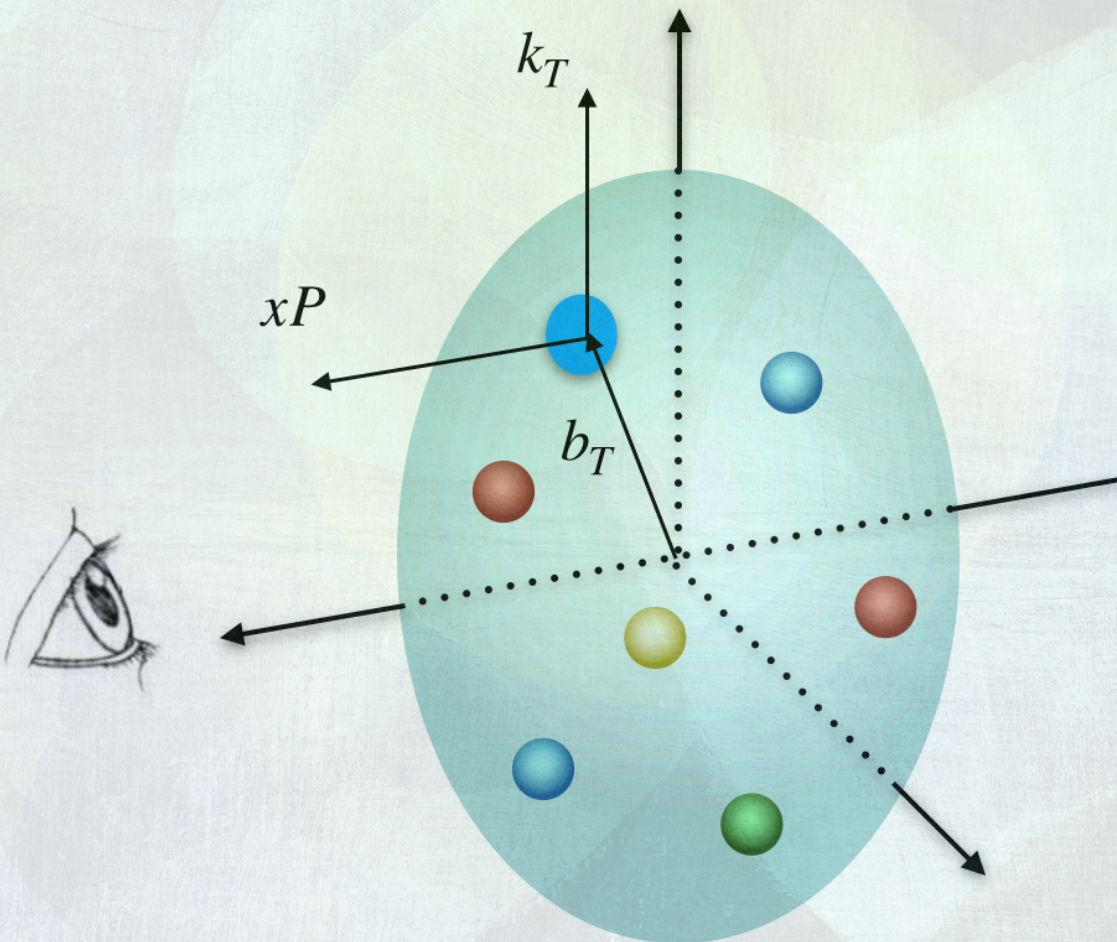
$$(e + p \rightarrow e' + X + n)$$

❖ Longitudinal structure ( $xP$ )

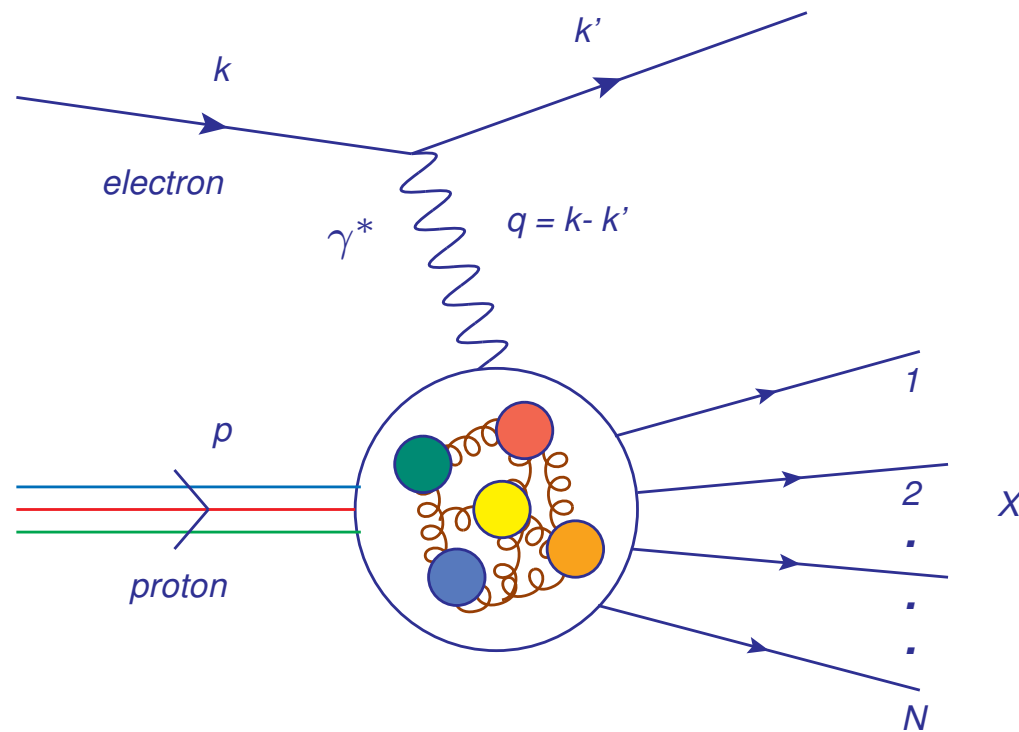
## ➤ Exclusive $J/\psi$ photo production with leading neutrons

$$(e + p \rightarrow e' + J/\psi + \pi + n)$$

❖ Transverse structure ( $b_T$ )

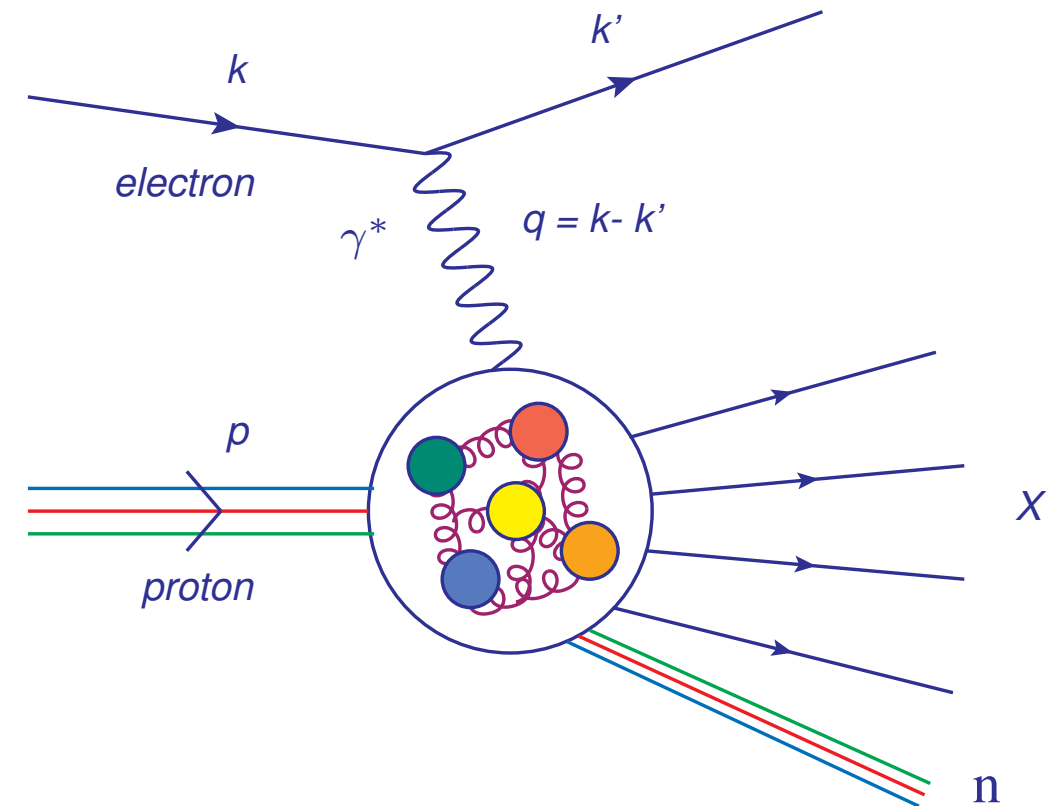


# INCLUSIVE DIS



- ❖ Detect the scattered electron
- ❖ Probe partonic structure of the targets
- ❖ Kinematic variables :  $x_{Bj}$ ,  $Q^2$ ,  $W$
- ❖ Precise measurements of the structure functions from HERA ( $F_2$ ,  $F_L$ )

# TAGGED DIS (TDIS)

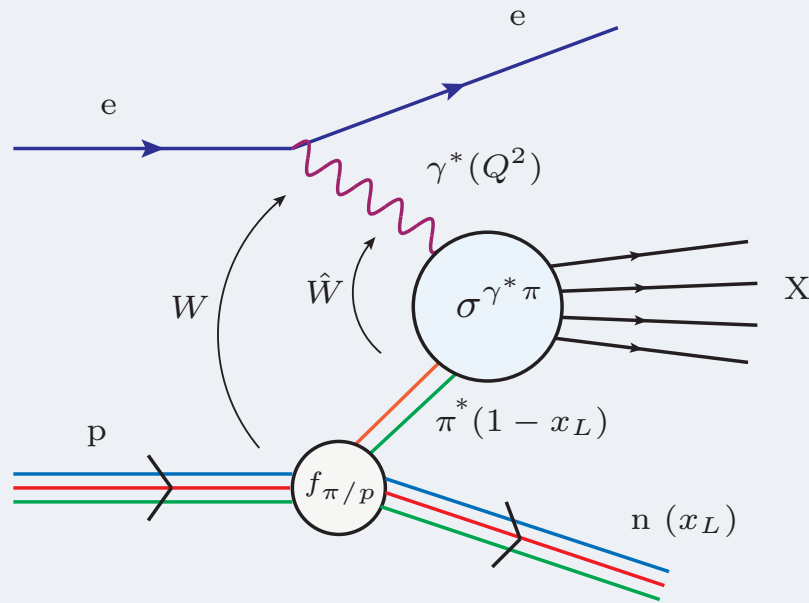


- ❖ Detect the scattered electron and the outgoing target nucleon
- ❖ Probe partonic structure of the “effective” targets not readily found
- ❖ Kinematic variables :  $x_{Bj}$ ,  $Q^2$ ,  $W$  and

$x_L \rightarrow$  momentum fraction carried by outgoing nucleon

$t \rightarrow$  four-momentum transfer squared at the nucleon vertex

# LEADING NEUTRONS (LN)



HI EPJC 74 (2014), 2915

## ❖ Forward neutrons:

$$\eta > 7.9, 0.1 < x_L < 0.94$$

$$0 < p_T < 0.6$$

## ❖ Kinematic variables:

$$\hat{x} = \frac{Q^2 + m_f^2}{\hat{W}^2 + Q^2} = \frac{Q^2 + m_f^2}{(1 - x_L)W^2 + Q^2}$$

$$t \simeq -\frac{p_T^2}{x_L} - (1 - x_L) \left( \frac{m_n^2}{x_L} - m_p^2 \right)$$

## ❖ LN Structure function $F_2^{LN}$ :

HI EPJC 68 (2010), 381

$$\frac{d^4 \sigma^{ep \rightarrow eXn}}{dx dQ^2 dx_L dt} = \frac{4\pi\alpha_{EM}^2}{xQ^4} \left( 1 - y + \frac{y^2}{2} \right) F_2^{LN(4)}(x, Q^2, x_L, t)$$

## ❖ In terms of $\gamma^*p$ cross section:

$$F_2^{LN}(x, Q^2, x_L) = \frac{Q^2}{4\pi^2\alpha_{EM}} \frac{d\sigma^{\gamma^*p \rightarrow Xn}}{dx_L}$$

J.D. Sullivan PRD 5 (1972), 1732

## ❖ In One Pion Exchange (OPE) approximation:

$$\frac{d^2 \sigma(W, Q^2, x_L, t)}{dx_L dt} = f_{\pi/p}(x_L, t) \sigma^{\gamma^*\pi^*}(\hat{W}^2, Q^2)$$

$f_{\pi/p}(x_L, t)$  is pion splitting function,

$\sigma^{\gamma^*\pi^*}(\hat{W}^2, Q^2)$  is virtual photon-virtual pion cross section

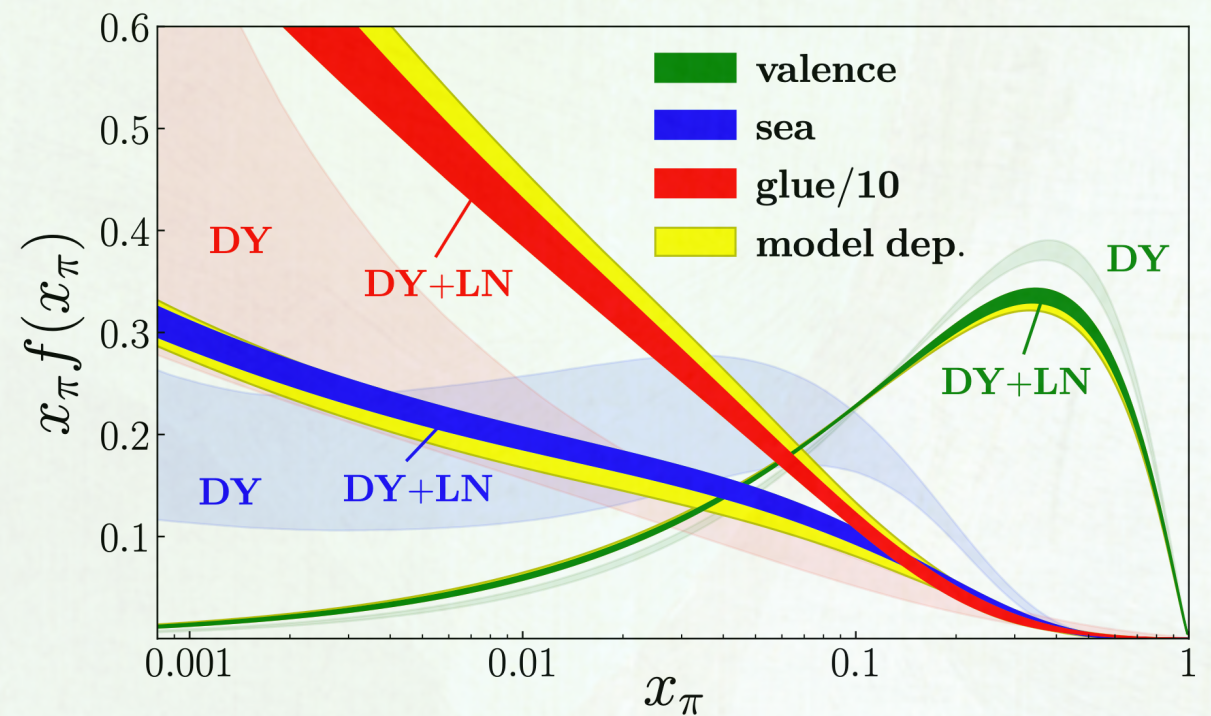
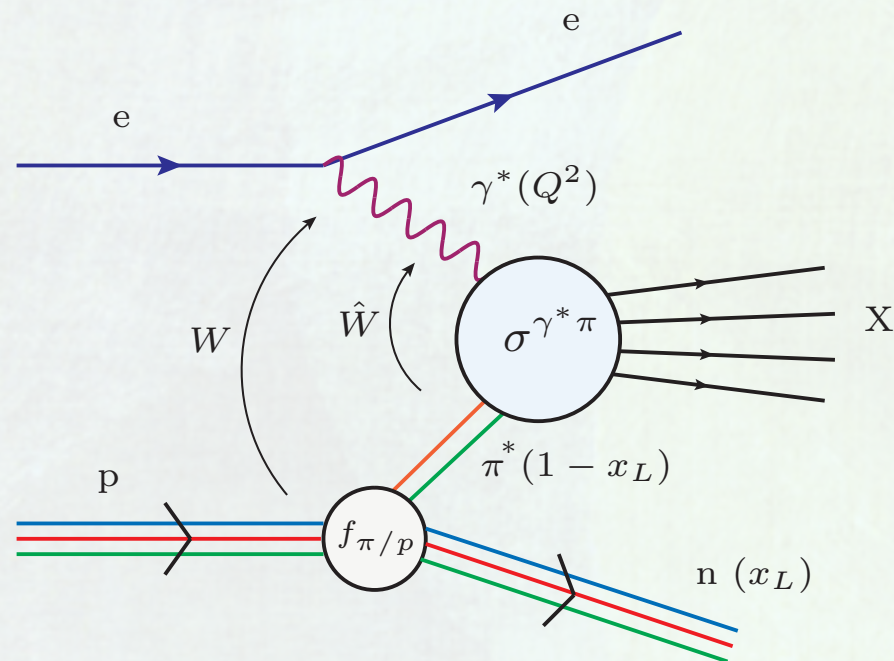
## ❖ OPE allows to extract the pion structure function $F_2^\pi$ ,

$$F_2^{LN}(W, Q^2, x_L) = \Gamma(x_L, Q^2) F_2^\pi(W, Q^2, x_L)$$

$\Gamma(x_L, Q^2)$  is t-integrated flux of pions from proton



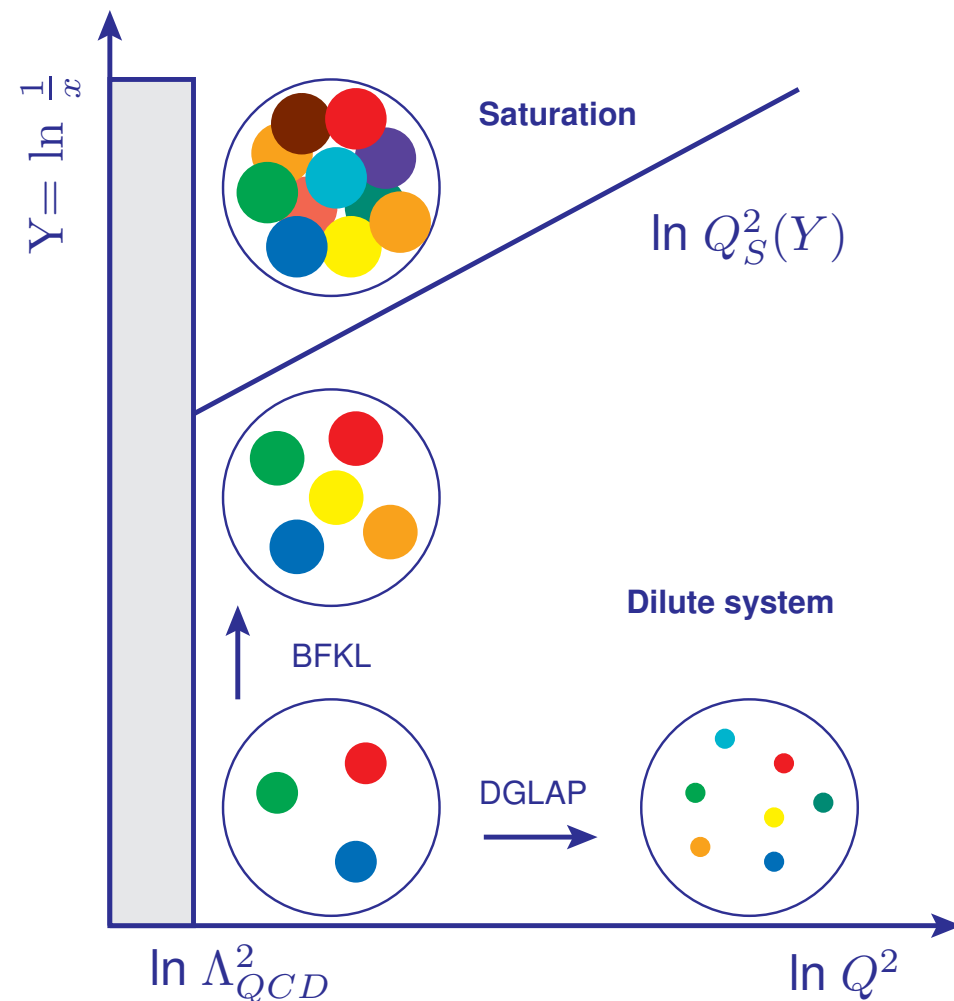
# INCLUSIVE MEASUREMENTS WITH LEADING NEUTRONS



Barry et al PRL 121 (2018), 152001

- ★ Universality between the pion and proton structure
- ★ Saturation effects and Geometric Scaling
- ★ Feynman- $x_L$  spectra and Feynman scaling

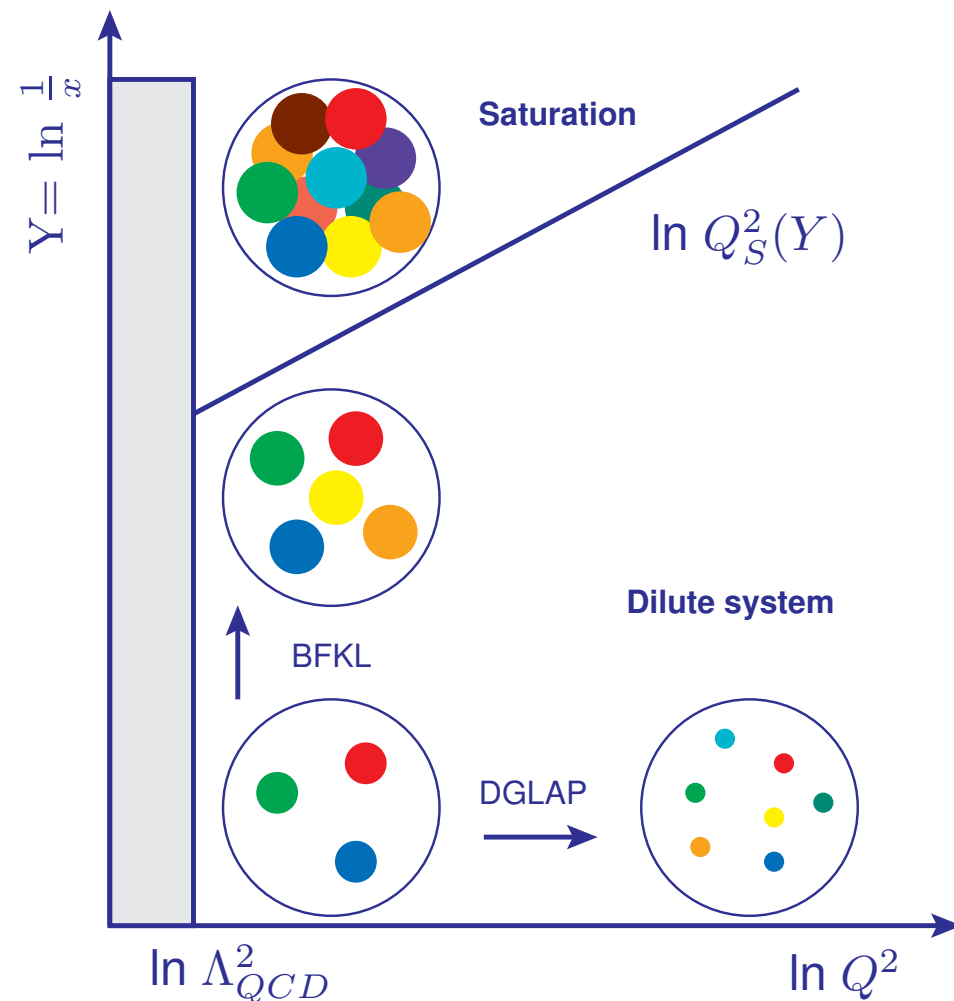
# QCD PHASE SPACE DIAGRAM



- ❖ Bjorken limit:  $Q^2 \rightarrow \infty, s \rightarrow \infty; x = \text{fixed}$ 
  - Phase space density ( $\# \text{partons}/\text{Area}/Q^2$ ) decreases
  - Target becomes dilute
- ❖ High energy limit:  $x \rightarrow 0, s \rightarrow \infty; Q^2 = \text{fixed}$ 
  - Phase space density ( $\# \text{partons}/\text{Area}/Q^2$ ) increases
  - Target becomes dense
- ❖ DGLAP & BFKL evolution equations violate unitarity
- ❖ High energy limit of QCD suggests presence of multi-body dynamics and non-linear physics

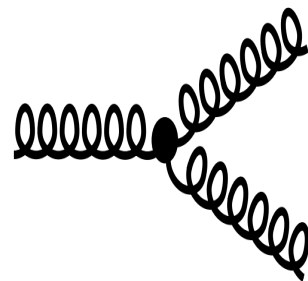


# QCD PHASE SPACE DIAGRAM

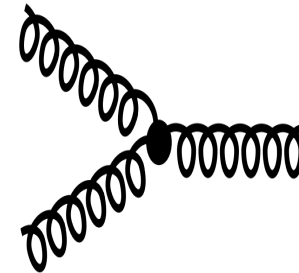


- ❖ Bjorken limit:  $Q^2 \rightarrow \infty, s \rightarrow \infty; x = \text{fixed}$ 
  - Phase space density ( $\# \text{partons}/\text{Area}/Q^2$ ) decreases
  - Target becomes dilute
- ❖ High energy limit:  $x \rightarrow 0, s \rightarrow \infty; Q^2 = \text{fixed}$ 
  - Phase space density ( $\# \text{partons}/\text{Area}/Q^2$ ) increases
  - Target becomes dense
- ❖ DGLAP & BFKL evolution equations violate unitarity
- ❖ High energy limit of QCD suggests presence of multi-body dynamics and non-linear physics

(Gluon emission)

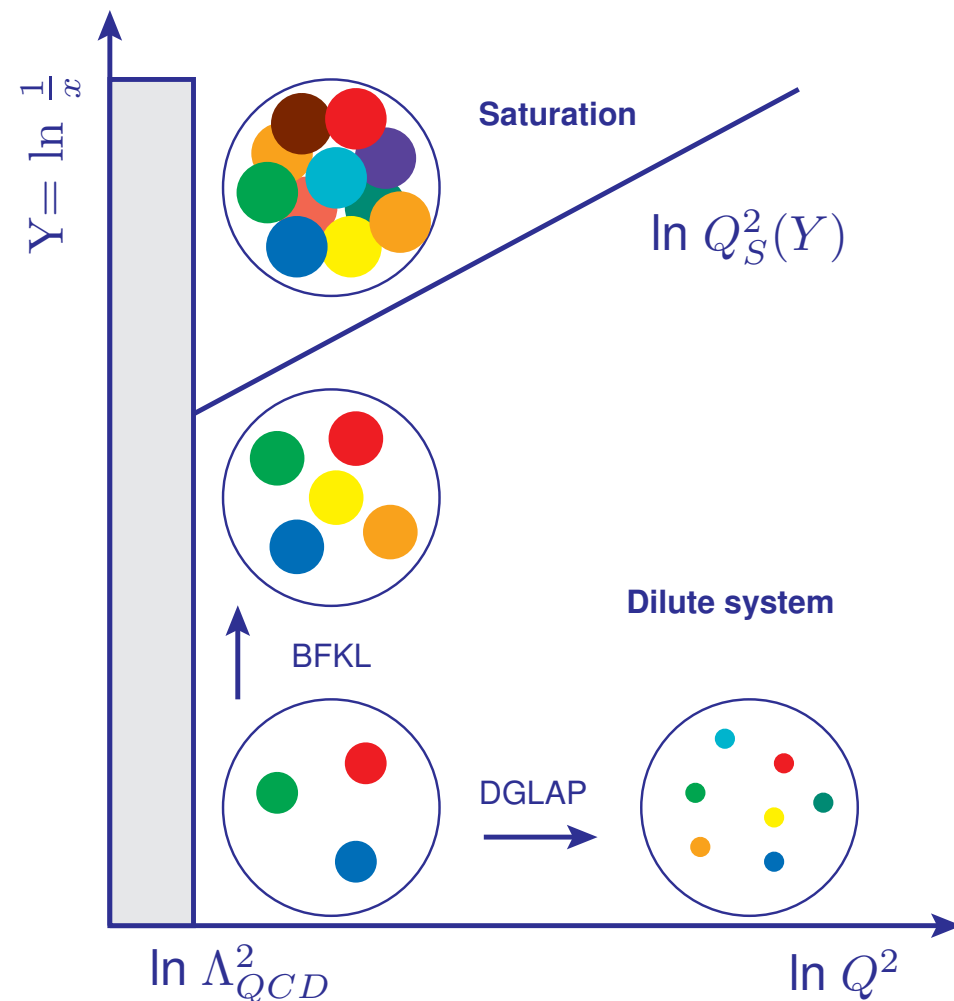


—



(Gluon recombination)

# QCD PHASE SPACE DIAGRAM



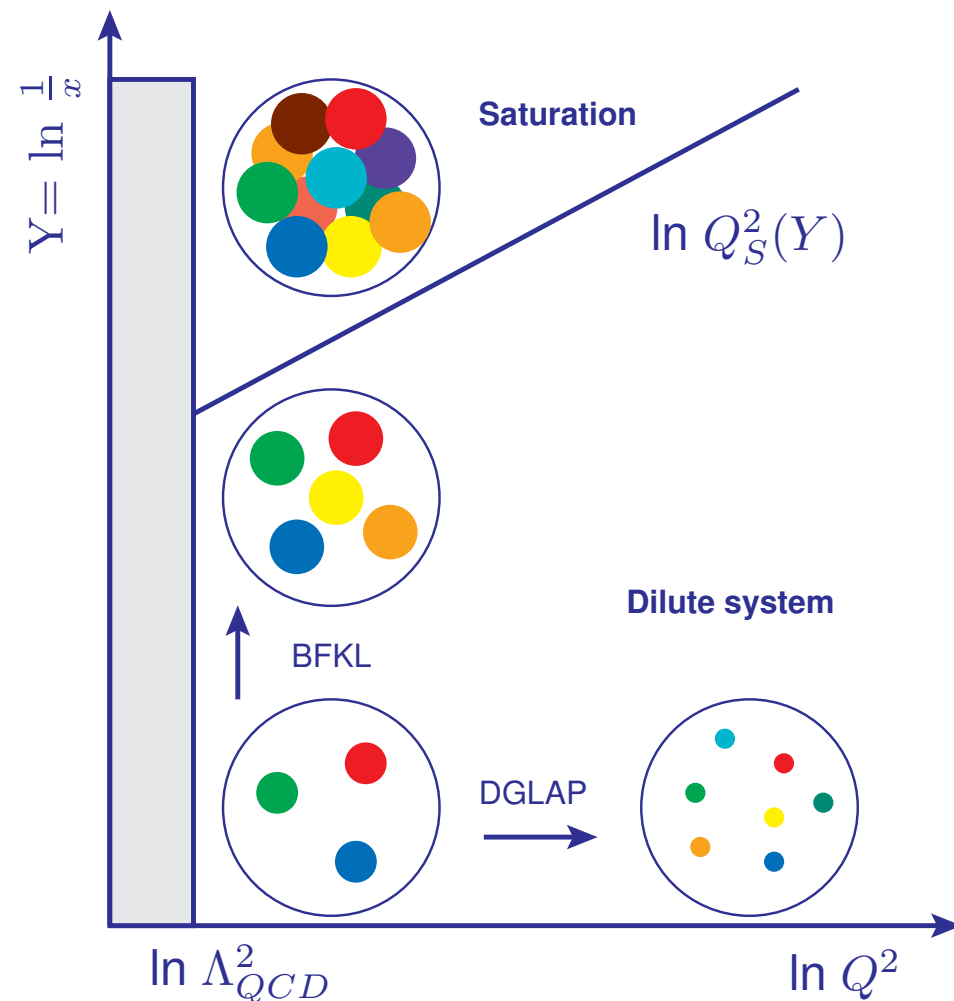
- ❖ Bjorken limit:  $Q^2 \rightarrow \infty, s \rightarrow \infty; x = \text{fixed}$ 
  - Phase space density ( $\# \text{partons}/\text{Area}/Q^2$ ) decreases
  - Target becomes dilute
- ❖ High energy limit:  $x \rightarrow 0, s \rightarrow \infty; Q^2 = \text{fixed}$ 
  - Phase space density ( $\# \text{partons}/\text{Area}/Q^2$ ) increases
  - Target becomes dense
- ❖ DGLAP & BFKL evolution equations violate unitarity
- ❖ High energy limit of QCD suggests presence of multi-body dynamics and non-linear physics

**Gluon Saturation:** The GLR-MQ equation Gribov, Levin. & Ryskin, Mueller & Qiu 1986

$$\frac{\partial^2 xg(x, Q^2)}{\partial \ln Q^2 \partial \ln(1/x)} = \frac{3\alpha_s}{\pi} xg(x, Q^2) - \frac{81\alpha_s^2}{16Q^2 R^2} (xg(x, Q^2))^2$$



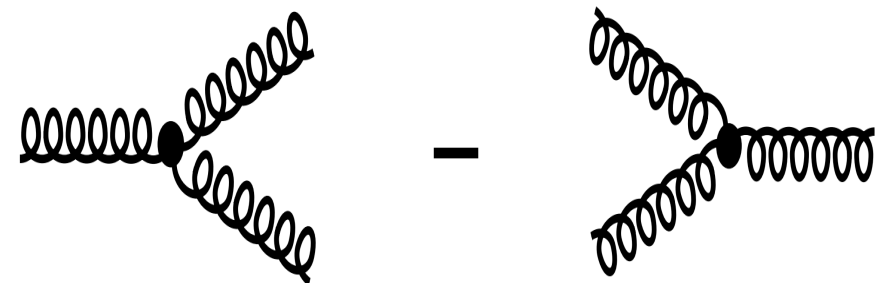
# QCD PHASE SPACE DIAGRAM



- ❖ Bjorken limit:  $Q^2 \rightarrow \infty, s \rightarrow \infty; x = \text{fixed}$ 
  - Phase space density ( $\# \text{partons}/\text{Area}/Q^2$ ) decreases
  - Target becomes dilute
- ❖ High energy limit:  $x \rightarrow 0, s \rightarrow \infty; Q^2 = \text{fixed}$ 
  - Phase space density ( $\# \text{partons}/\text{Area}/Q^2$ ) increases
  - Target becomes dense
- ❖ DGLAP & BFKL evolution equations violate unitarity
- ❖ High energy limit of QCD suggests presence of multi-body dynamics and non-linear physics

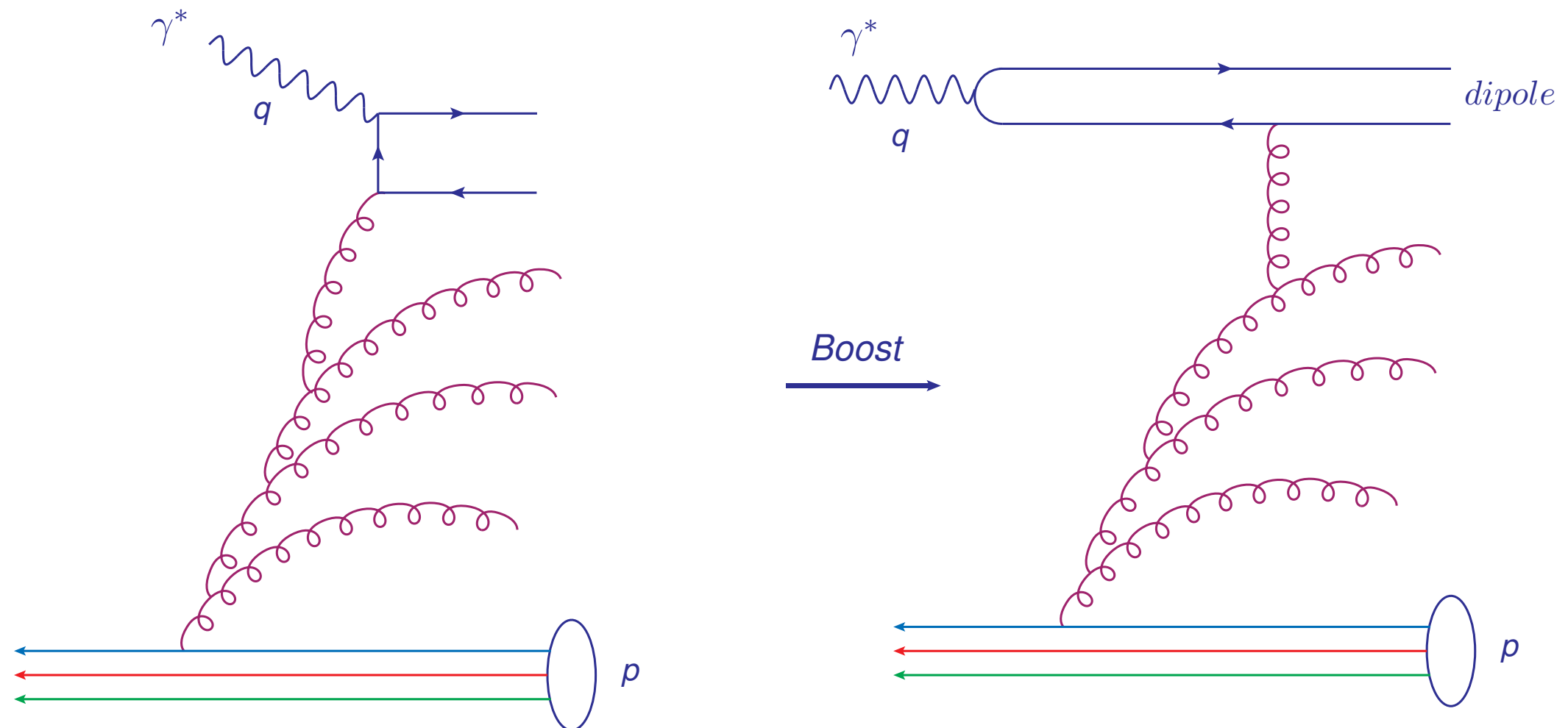
**Gluon Saturation:** The GLR-MQ equation

$$\frac{\partial^2 xg(x, Q^2)}{\partial \ln Q^2 \partial \ln(1/x)} = \frac{3\alpha_s}{\pi} xg(x, Q^2) - \frac{81\alpha_s^2}{16Q^2 R^2} (xg(x, Q^2))^2$$



# THE DIPOLE FRAME

---

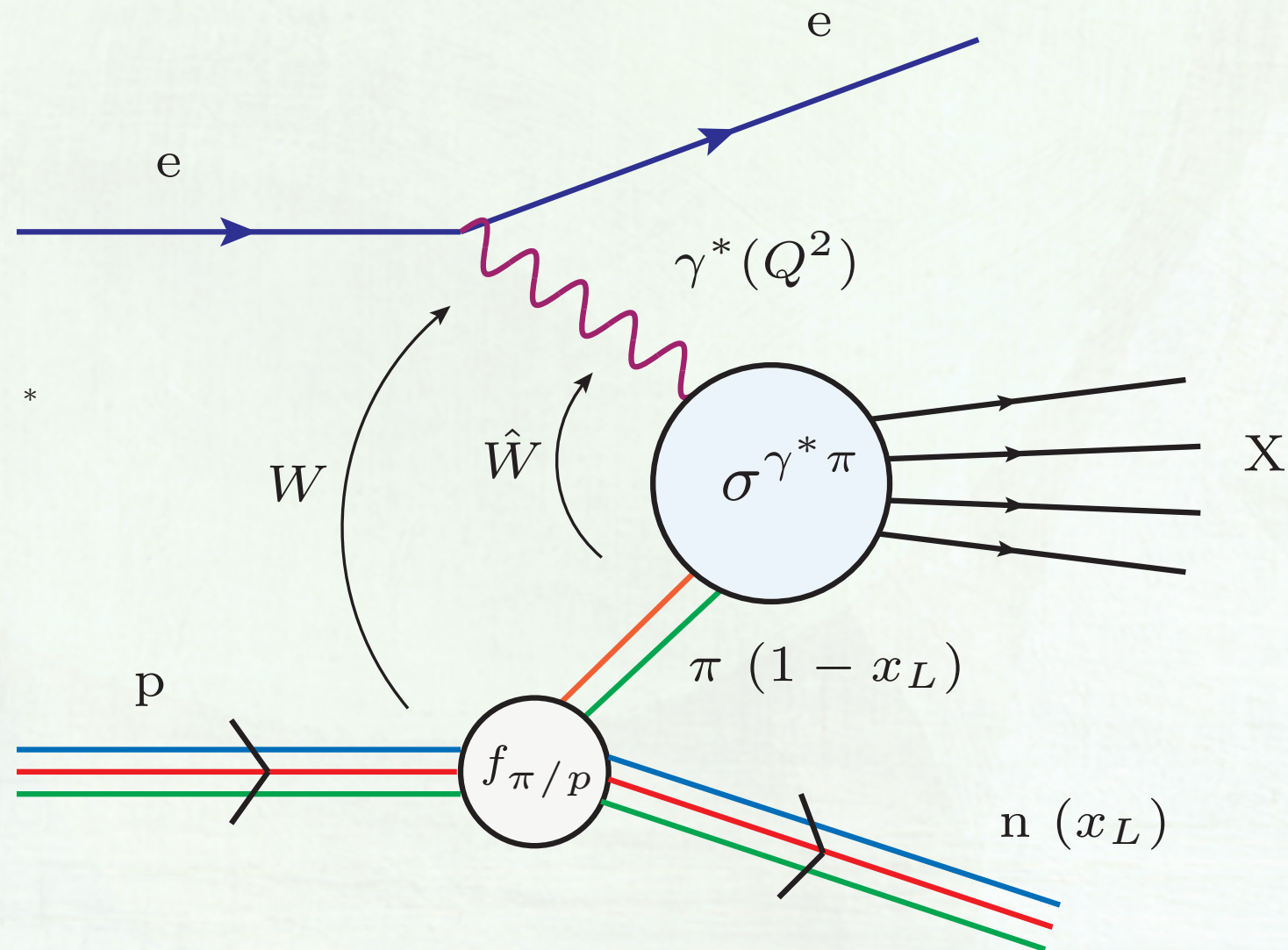


- ❖ Physical picture of DIS depends upon frame but the physical observables are independent of it
- ❖ Parton picture manifest in infinite momentum frame (IMF) & High energy limit better analysed in the dipole frame
- ❖ Dipole frame : the recombination effects (non linear evolution) gets mapped to linear evolution + multiple scatterings



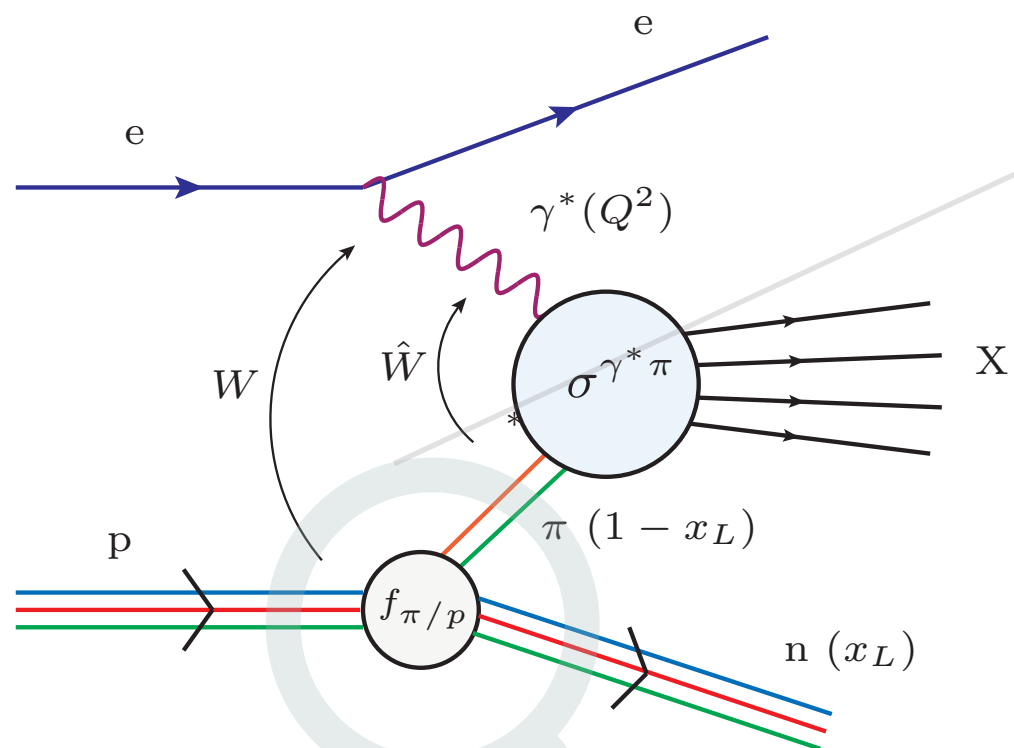
# INCLUSIVE CROSS SECTION WITH LEADING NEUTRONS

---



# PION FLUX FROM PROTON

---





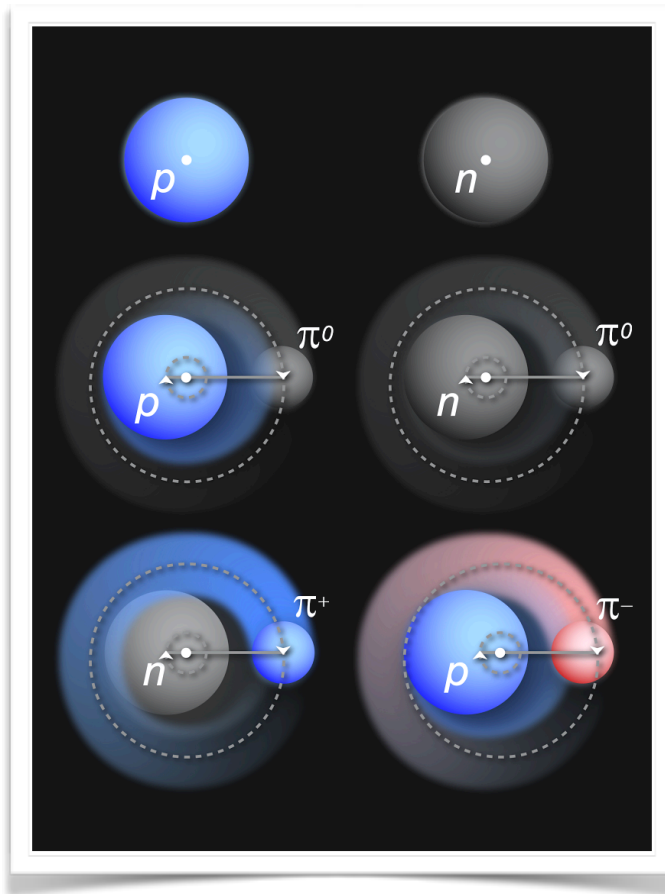
# PION FLUX FROM PROTON

Chiral approach:  $a=0.24$ ,  $b=0.12$   
Thomas, Melnitchouk & Steffens,  
PRL85 (2000) 2892

- ❖ Proton as a superposition of states in meson-cloud models,

$$|p\rangle \rightarrow \sqrt{1-a-b} |p_o\rangle + \sqrt{a} \left( -\sqrt{\frac{1}{3}} |p_0 \pi^0\rangle + \sqrt{\frac{2}{3}} |n_0 \pi^+\rangle \right) + \sqrt{b} \left( -\sqrt{\frac{1}{2}} |\Delta_0^{++} \pi^-\rangle - \sqrt{\frac{1}{3}} |\Delta_0^+ \pi^0\rangle + \sqrt{\frac{1}{6}} |\Delta_0^0 \pi^+\rangle \right)$$

- ❖ Pion flux from proton is well known & can be calculated using chiral effective theory
- ❖ Previously used to explain hadron-hadron interactions at LHC



- ❖ We use the following flux factor: [Carvalho et al PLB 752 \(2016\) 76](#)

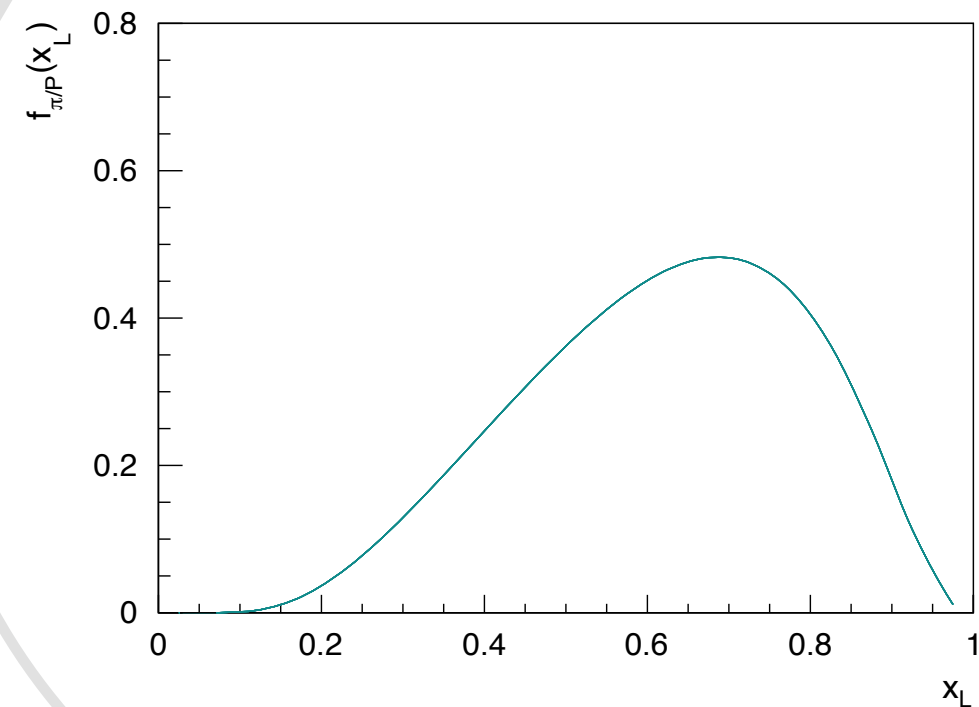
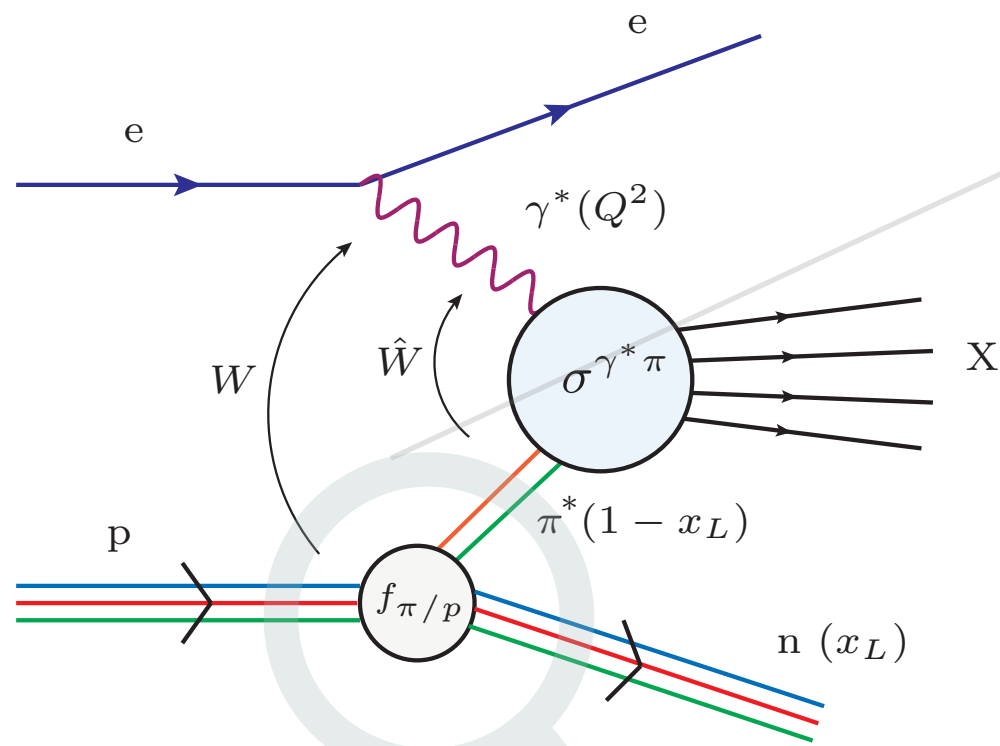
$$f_{\pi/p}(x_L, t) = \frac{1}{4\pi} \frac{2g_{p\pi p}^2}{4\pi} \frac{|t|}{(m_\pi^2 + |t|)^2} (1 - x_L)^{1-2\alpha(t)} [F(x_L, t)]^2$$

where the form factor is given by:

$$F(x_L, t) = \exp \left[ -R^2 \frac{|t| + m_\pi^2}{(1 - x_L)} \right], \alpha(t) = 0$$

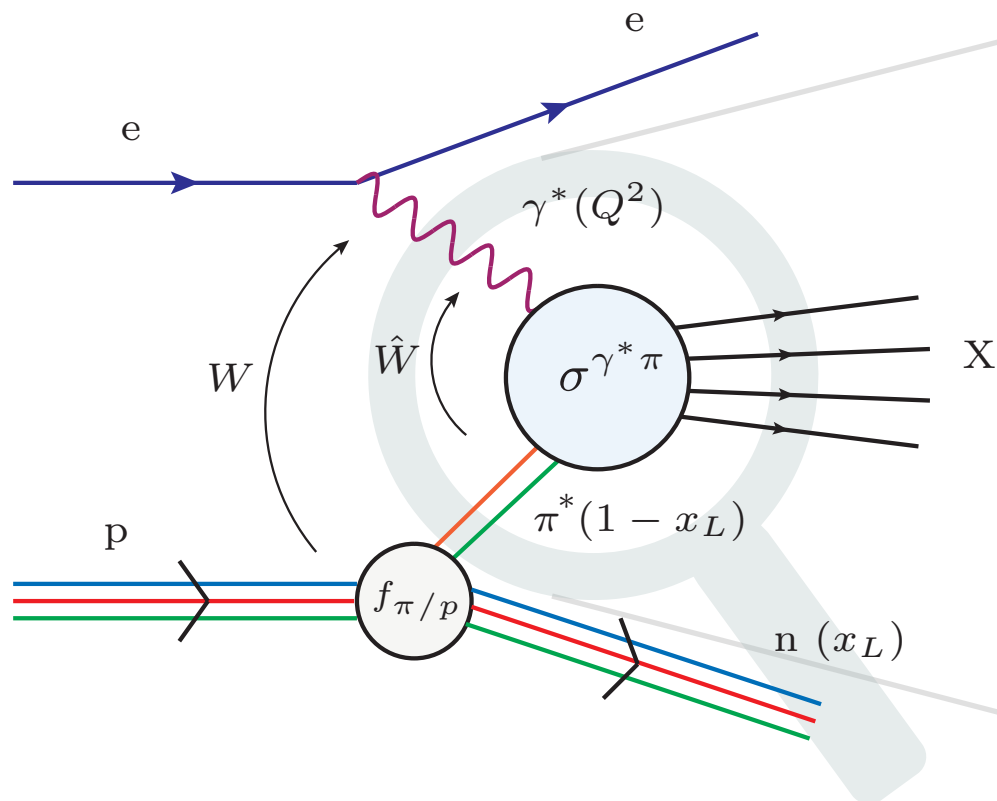
- ❖ Used by H1 and ZEUS for the data analysis [H1 EPJC 68 \(2010\), 381](#)

# PION FLUX FROM PROTON



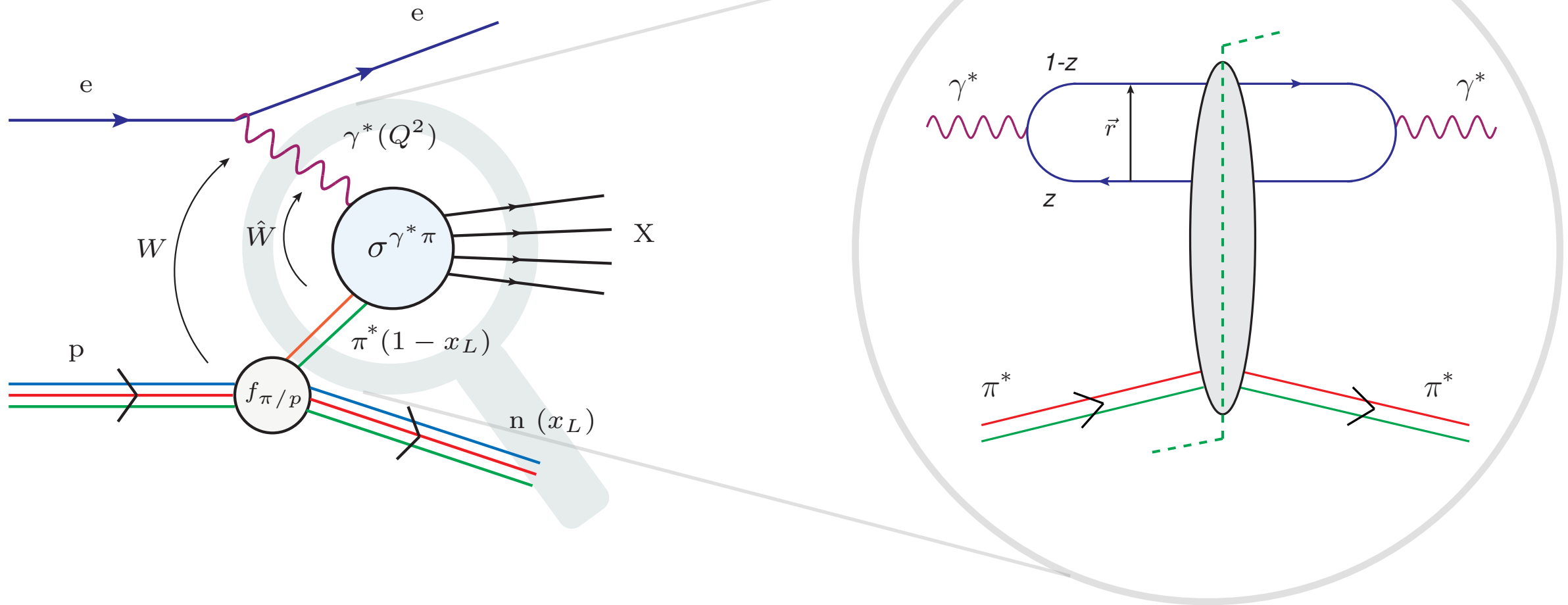
- ❖ The pion flux peaks at  $x_L \sim 0.7$ , which suggests that the LN spectra should also peak at high-  $x_L$  values

# VIRTUAL PION-PHOTON CROSS SECTION



- ❖ For total virtual photon- virtual pion cross section
  - use dipole framework (natural in target rest frame)

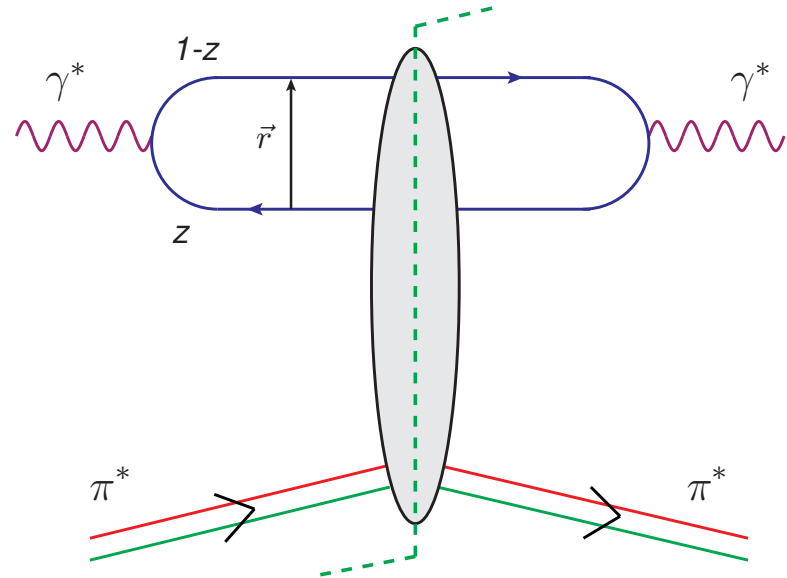
# VIRTUAL PION-PHOTON CROSS SECTION IN DIPOLE MODEL



- ❖ For total virtual photon- virtual pion cross section
  - use dipole framework (natural in target rest frame)



# VIRTUAL PION-PHOTON CROSS SECTION IN DIPOLE MODEL



Various stages of semi-inclusive scattering of photons on pions in dipole model:

1.  $\gamma^* \rightarrow q\bar{q}$  splitting (*QED*)
2. Dipole  $\rightarrow \pi^*$  scattering (*model + QCD*)
3. Dipole  $\rightarrow \gamma^*$  (*QED*)

$$\sigma_{L,T}^{\gamma^*\pi^*}(\hat{x}, Q^2) = \text{Im } \mathcal{A}(\hat{x}, Q^2, \Delta = 0) = \int d^2\mathbf{b} \int d^2\mathbf{r} \int \frac{dz}{4\pi} |\Psi_{L,T}^f(\mathbf{r}, z, Q^2)|^2 \frac{d\sigma_{q\bar{q}}^{(\pi)}}{d^2\mathbf{b}}(\mathbf{b}, \mathbf{r}, \hat{x})$$

❖ Two phenomenological parameterisations:

bSat :  $\frac{d\sigma_{q\bar{q}}^{(\pi)}}{d^2\mathbf{b}}(\mathbf{b}, \mathbf{r}, \hat{x}) = 2 \left[ 1 - \exp \left( - \frac{\pi^2}{2N_C} r^2 \alpha_s(\mu^2) \hat{x} g(\hat{x}, \mu^2) T_\pi(\mathbf{b}) \right) \right]$

bNonSat :  $\frac{d\sigma_{q\bar{q}}^{(\pi)}}{d^2\mathbf{b}}(\mathbf{b}, \mathbf{r}, \hat{x}) = \frac{\pi^2}{N_C} r^2 \alpha_s(\mu^2) \hat{x} g(\hat{x}, \mu^2) T_\pi(\mathbf{b})$  with

with  $T_\pi(b) = \frac{1}{2\pi B_\pi} e^{-\frac{b^2}{2B_\pi}}$  and  $\hat{x}g(\hat{x}, \mu_0^2) = A_g \hat{x}^{-\lambda_g} (1 - \hat{x})^2$  and  $\mu^2 = \mu_0^2 + \frac{C}{r^2}$ , the parameters  $A_g$ ,  $\lambda_g$ ,  $C$  are fitted to

leading neutron structure function HERA data.

# VIRTUAL PION-PHOTON CROSS SECTION IN DIPOLE MODEL

$$\sigma_{L,T}^{\gamma^*\pi^*}(\hat{x}, Q^2) = \text{Im } \mathcal{A}(\hat{x}, Q^2, \Delta = 0) = \int d^2\mathbf{b} \int d^2\mathbf{r} \int \frac{dz}{4\pi} |\Psi_{L,T}^f(\mathbf{r}, z, Q^2)|^2 \frac{d\sigma_{q\bar{q}}^{(\pi)}}{d^2\mathbf{b}}(\mathbf{b}, \mathbf{r}, \hat{x})$$

❖ Two approaches:

- Do a new fit of the dipole model parameters (  $A_g$ ,  $\lambda_g$ ,  $C$  ) to the LN Structure function data
- Use an assumption that the dipole-proton and dipole-pion cross section are related to each other

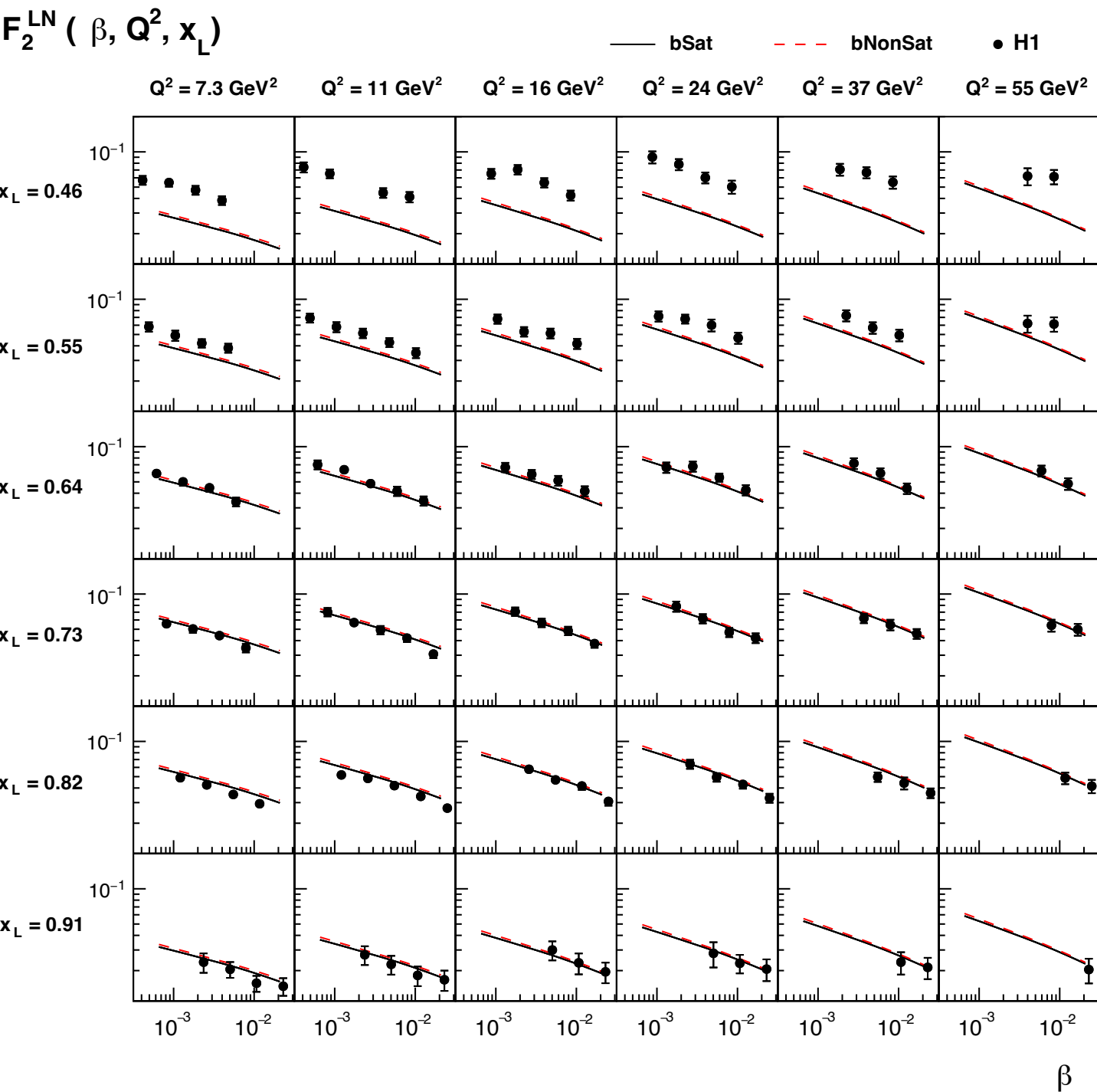
$$\frac{d\sigma_{q\bar{q}}^{(\pi)}}{d^2\mathbf{b}}(\mathbf{b}, \mathbf{r}, \beta) = R_q \frac{d\sigma_{q\bar{q}}^{(p)}}{d^2\mathbf{b}}(\mathbf{b}, \mathbf{r}, \beta) \quad ( \beta = \hat{x} )$$

$R_q$  is determined through fit to the LN structure function data and dipole-proton cross section is already known from the fit of dipole models to the reduced cross section data in inclusive DIS.

- Energy Dependence of dipole-pion and dipole-proton cross section is identical
- In constituent quark picture,  $R_q$  is ratio of number quarks in pion and proton i.e  $R_q = 2/3$

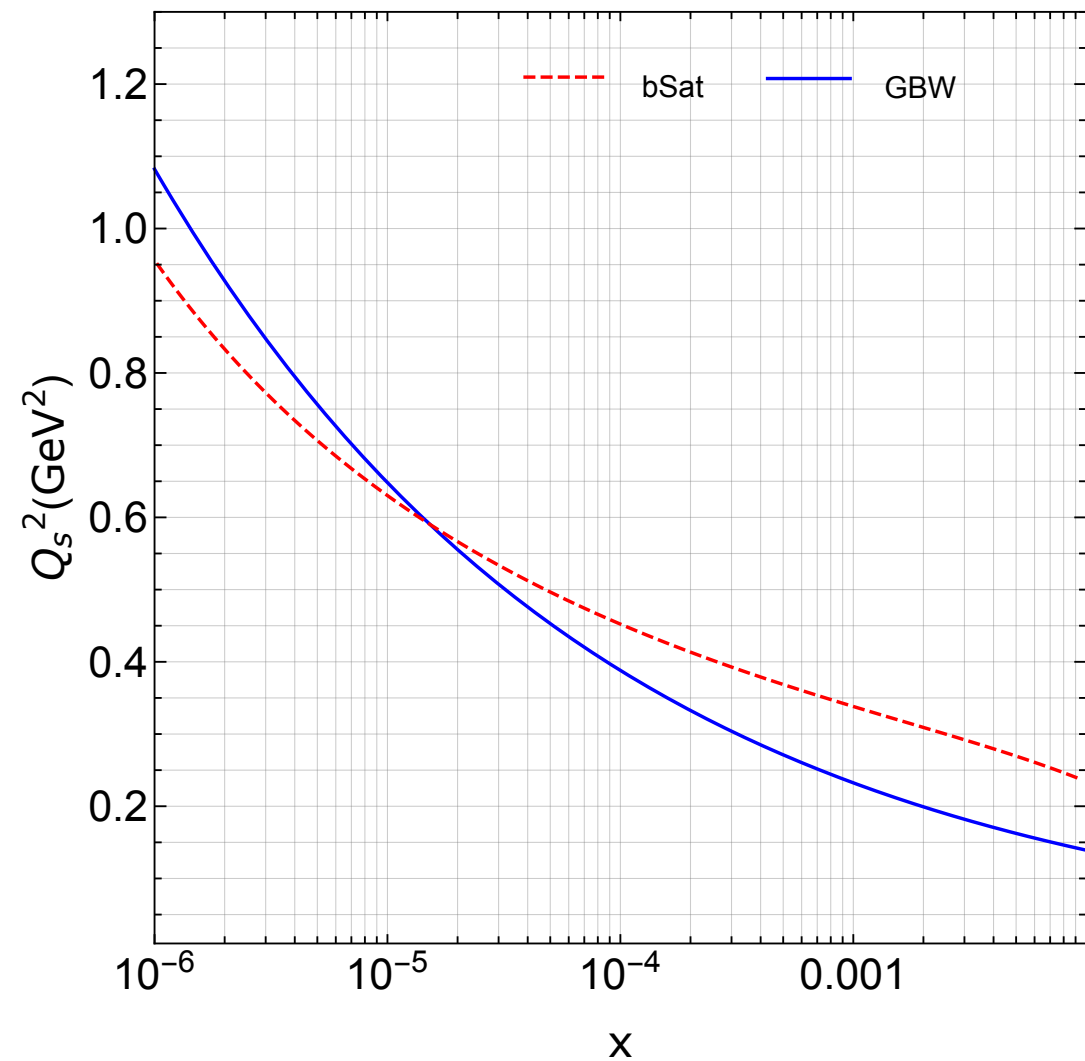
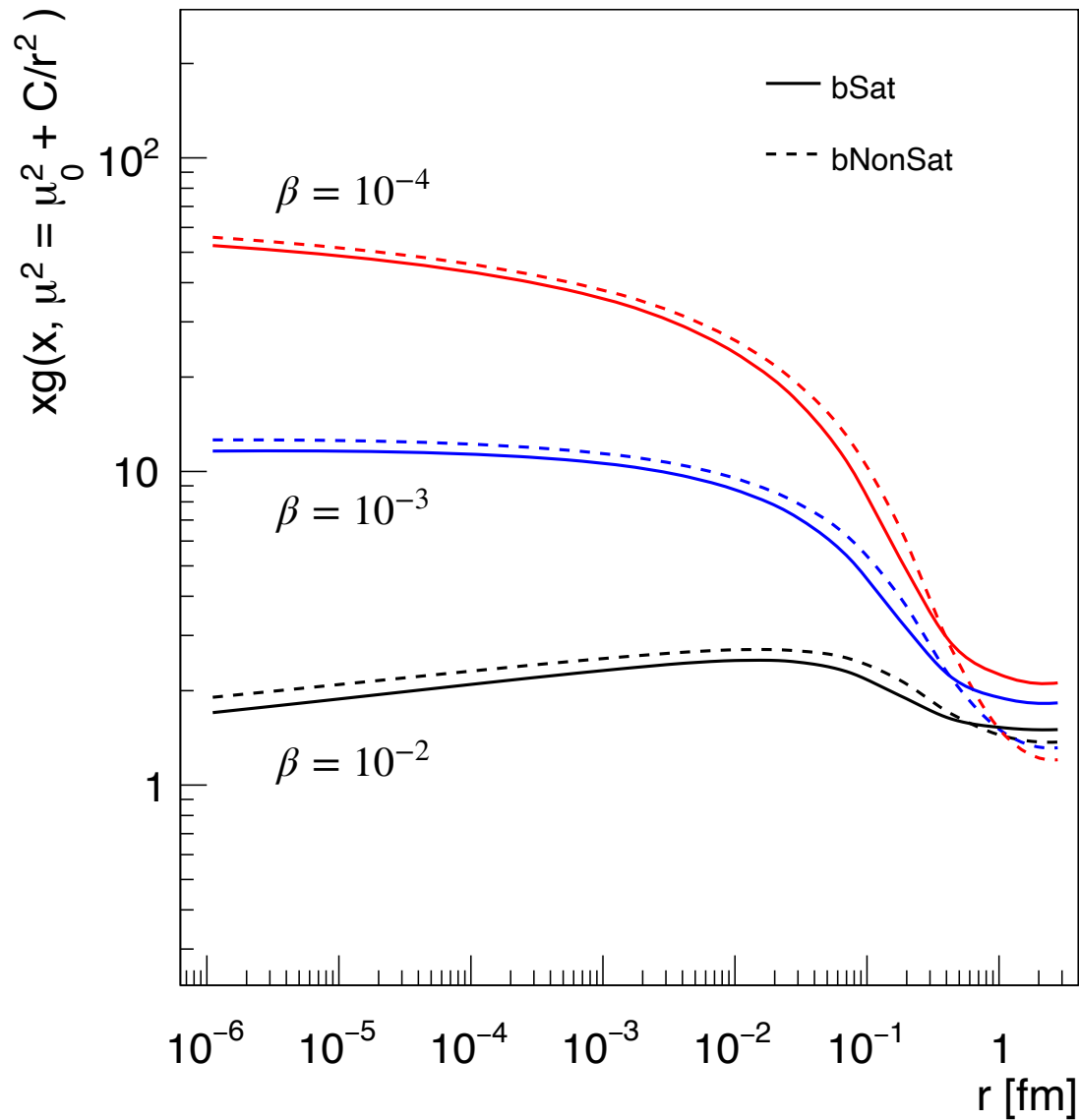
❖ We employ both the approaches and test the universality of pion and proton structure at small-x

# LN STRUCTURE FUNCTION $F_2^{LN}$



Fit	Model	C	$A_g$	$\lambda_g$	$R_q$	$\chi^2/N_{dof}$
1	bSat	$1.453 \pm 0.024$	$1.208 \pm 0.012$	$0.0600 \pm 0.0380$	—	$58.75/48 = 1.22$
2	bNonSat	$3.683 \pm 0.436$	$1.799 \pm 0.710$	$-0.0477 \pm 0.0038$	—	$57.61/48 = 1.20$
3	bSat	2.289	2.195	0.0829	$0.520 \pm 0.006$	$66.19/50 = 1.32$

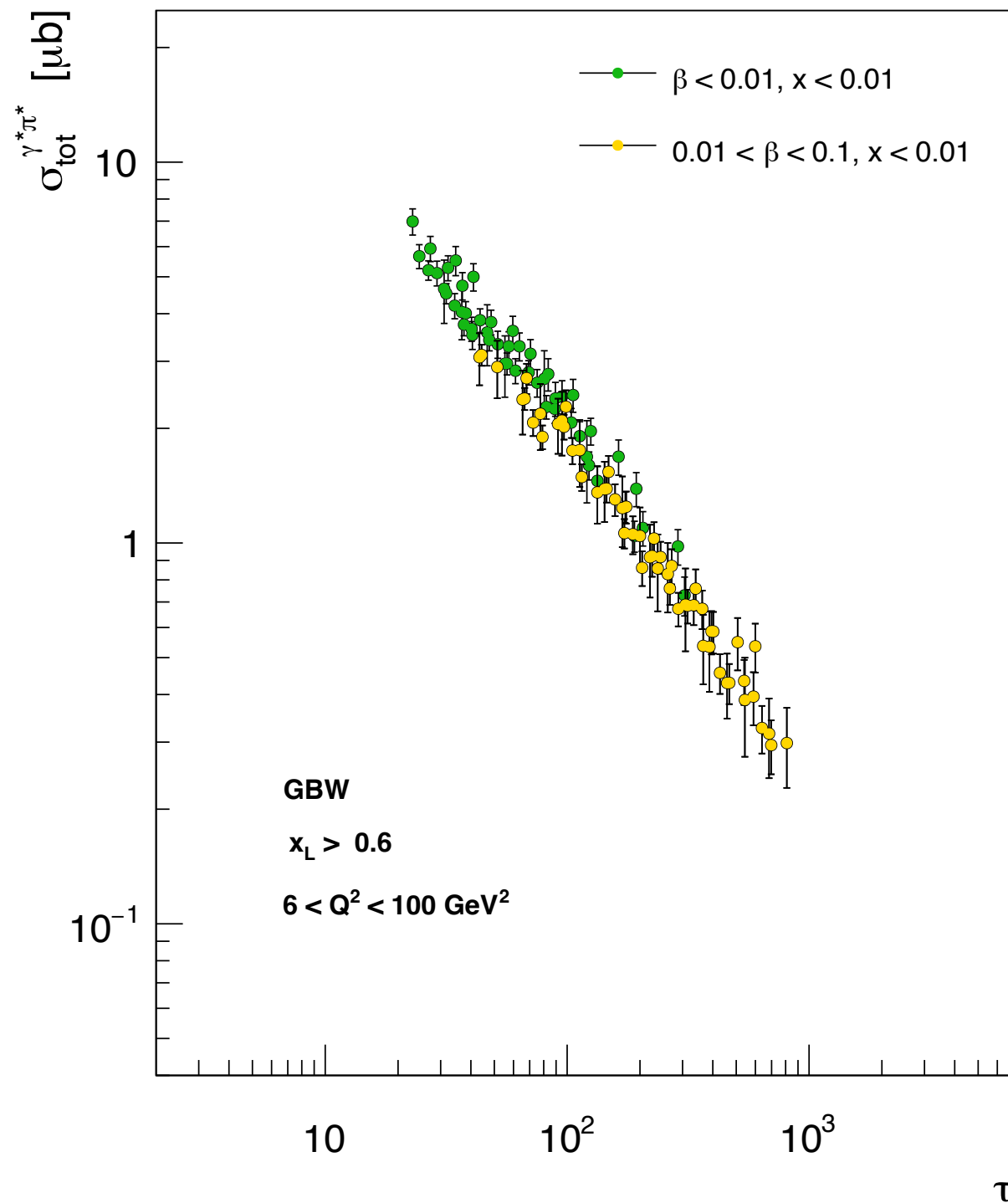
# GLUON DENSITY & SATURATION SCALE



- ❖ The initial condition effects are washed out in the evolution and gluon density is same for both the saturated and non-saturated dipole models.
- ❖ Saturation scale increases with decreasing  $x$  and reaches  $Q_s^2 \sim 1 \text{ GeV}^2$  for  $x \sim 10^{-6}$

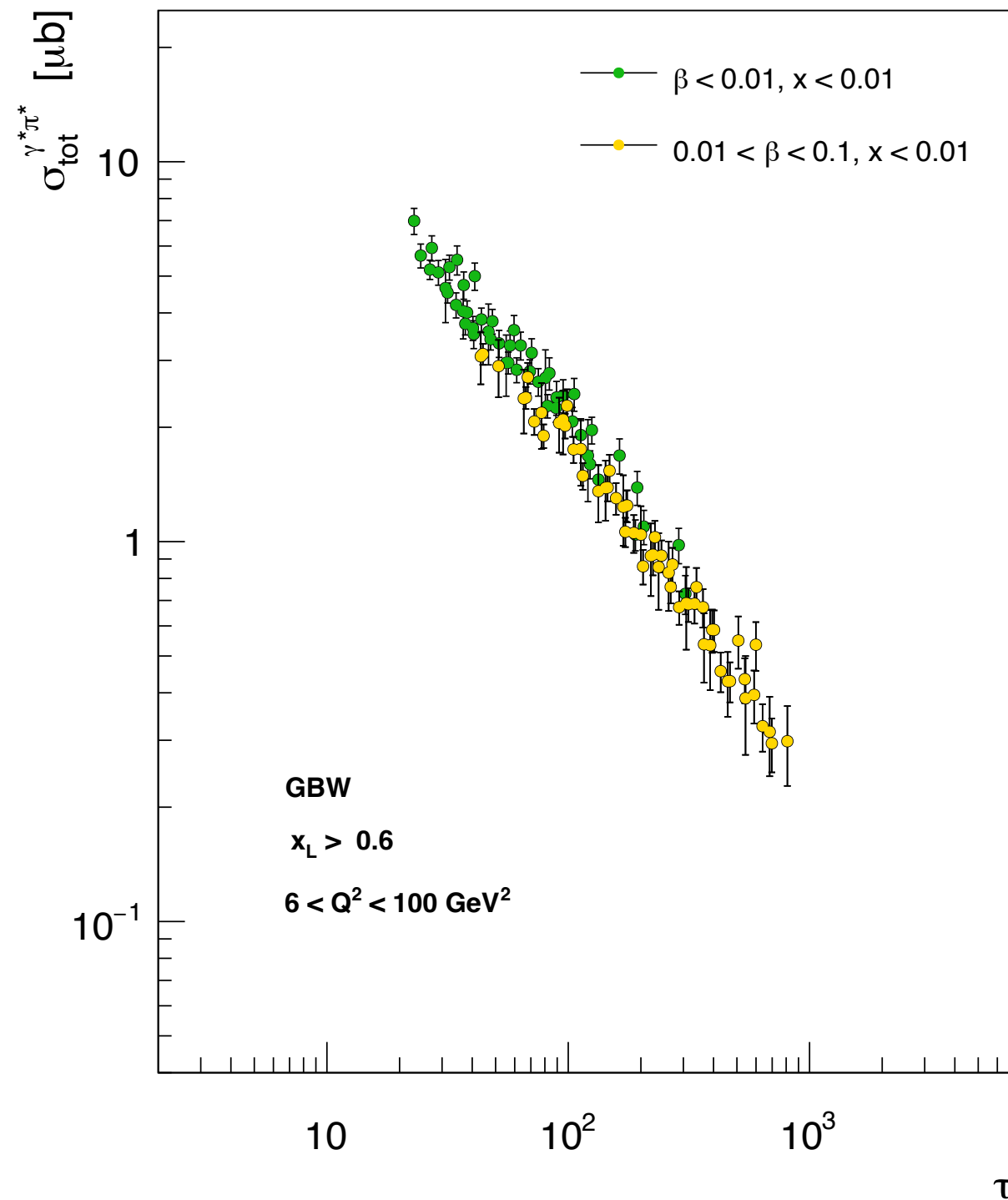


# GEOMETRIC SCALING





- ◆ The total cross section shows geometric scaling when plotted against  $\tau = \frac{Q^2}{Q_s^2(\beta)}$
- ◆ Can we say that the data shows saturation?
- ◆ Emergence of a scale  $Q_s^2(\beta)$  in data

# GEOMETRIC SCALING

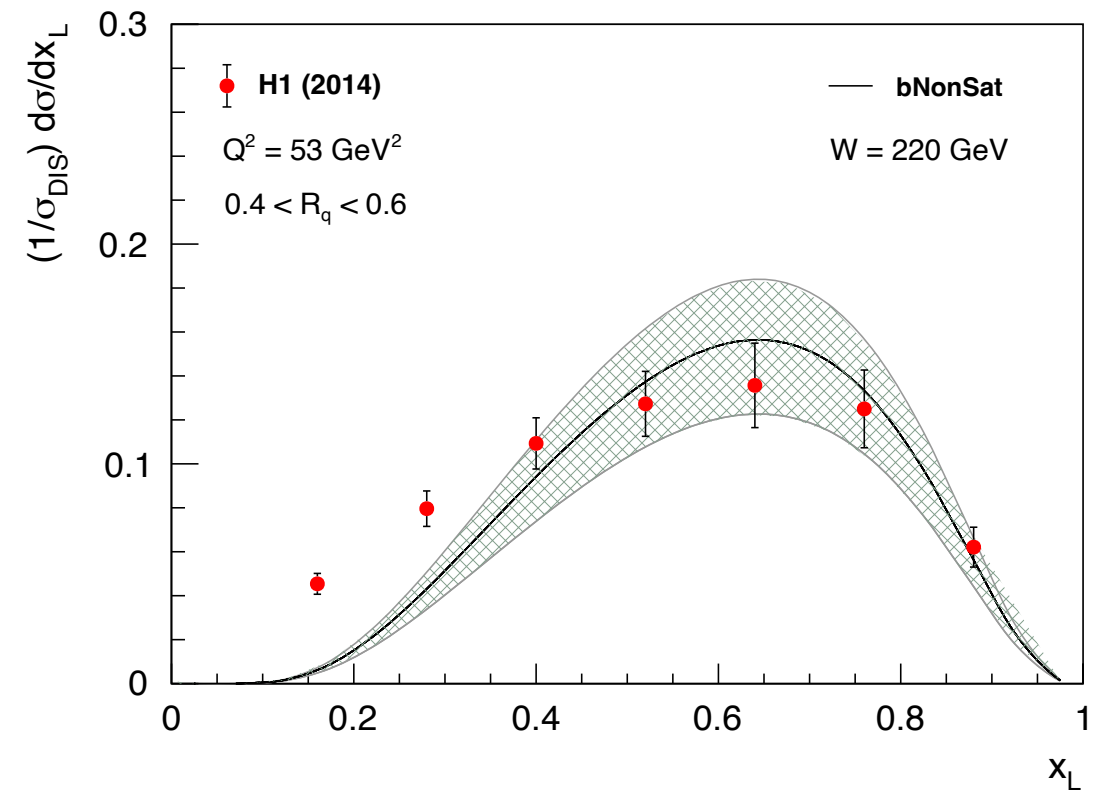
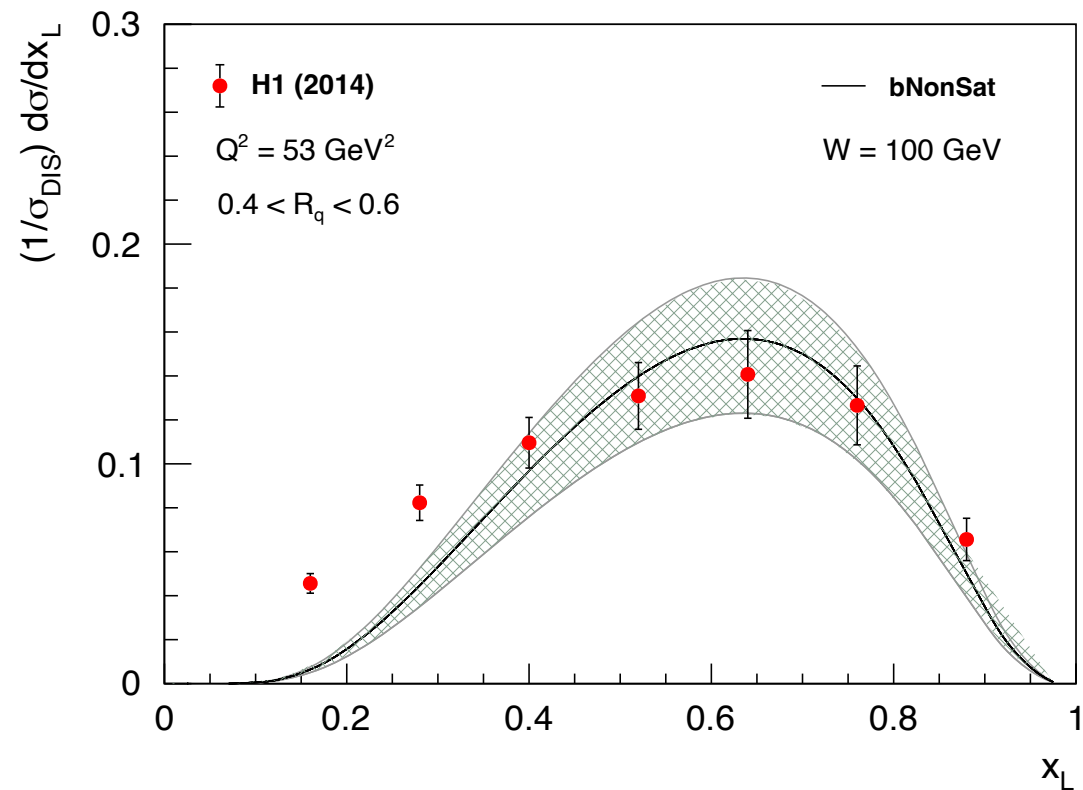
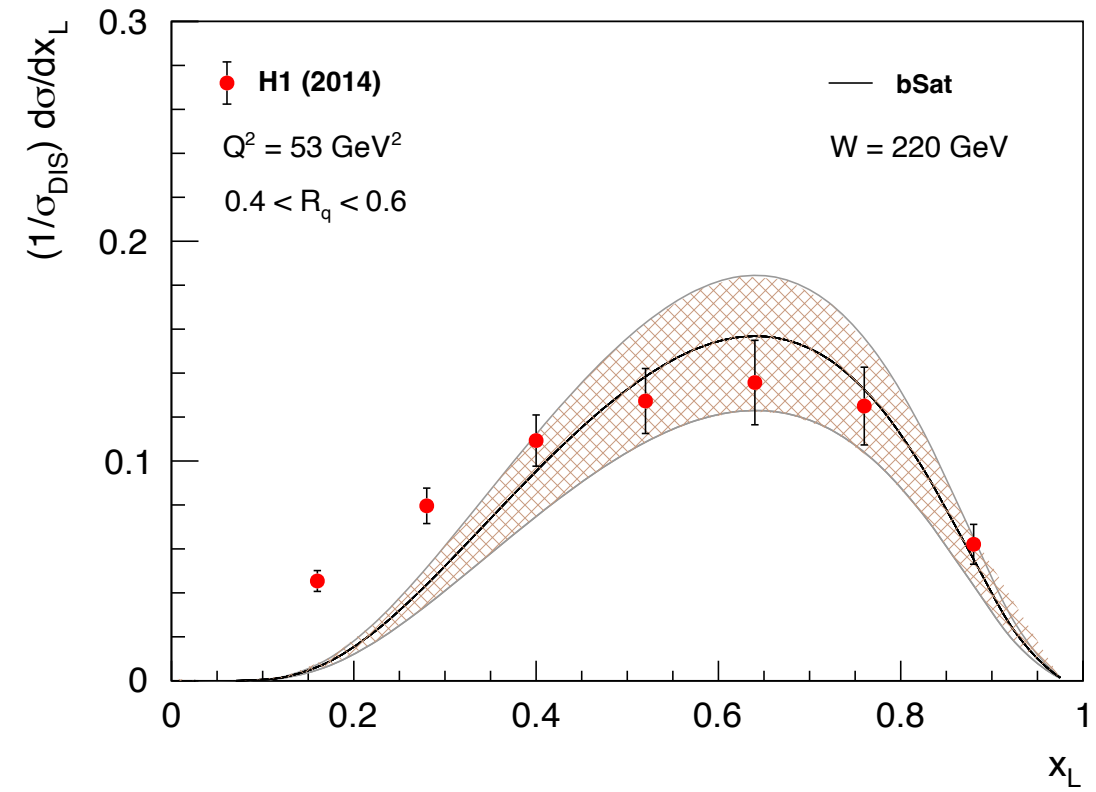
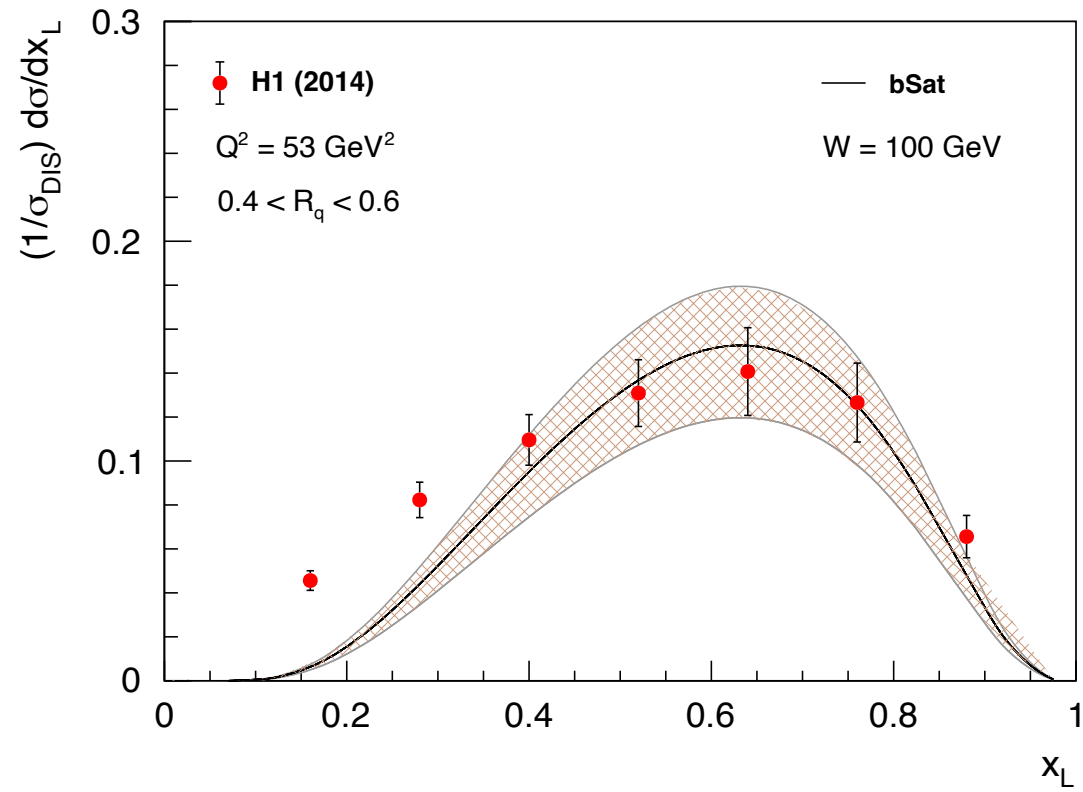


◆ The total cross section shows geometric scaling when plotted against  $\tau = \frac{Q^2}{Q_s^2(\beta)}$

◆ Can we say that the data shows saturation? 

◆ Emergence of a scale  $Q_s^2(\beta)$  in data 

# FEYNMAN-X SPECTRA

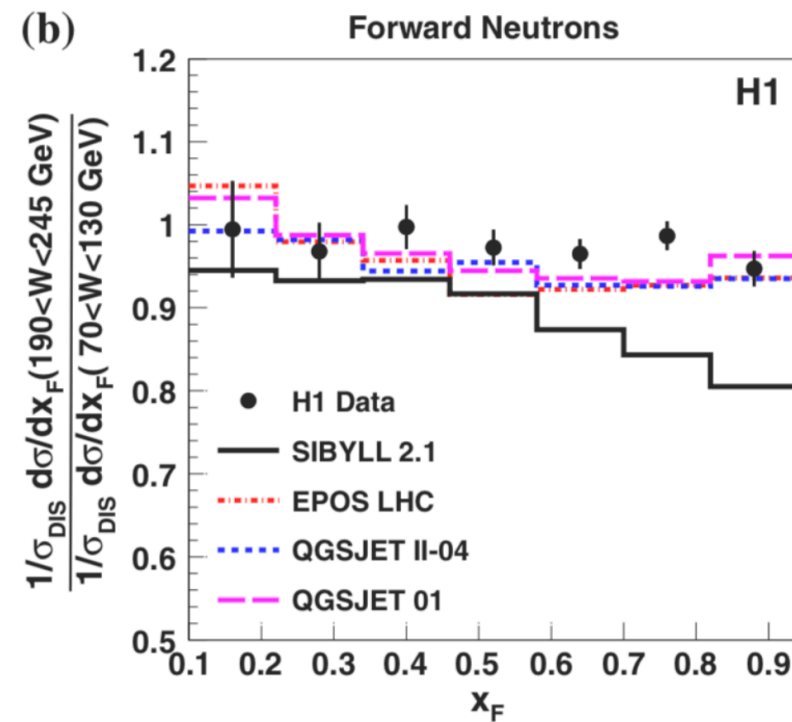
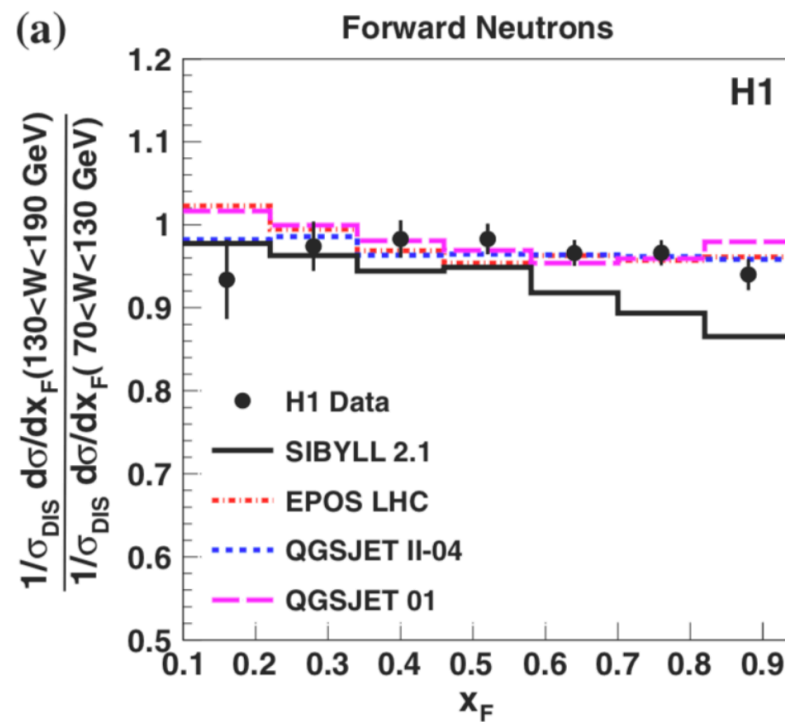




# SCALING IN FEYNMAN-X SPECTRA

- ❖ Proposed by Feynman long back using general behaviour of cross sections of hadrons at high energy
- ❖ H1 Data shows this scaling (*w.r.t*  $W$  &  $Q^2$ ) behaviour

H1 EPJC 74 (2014), 2915

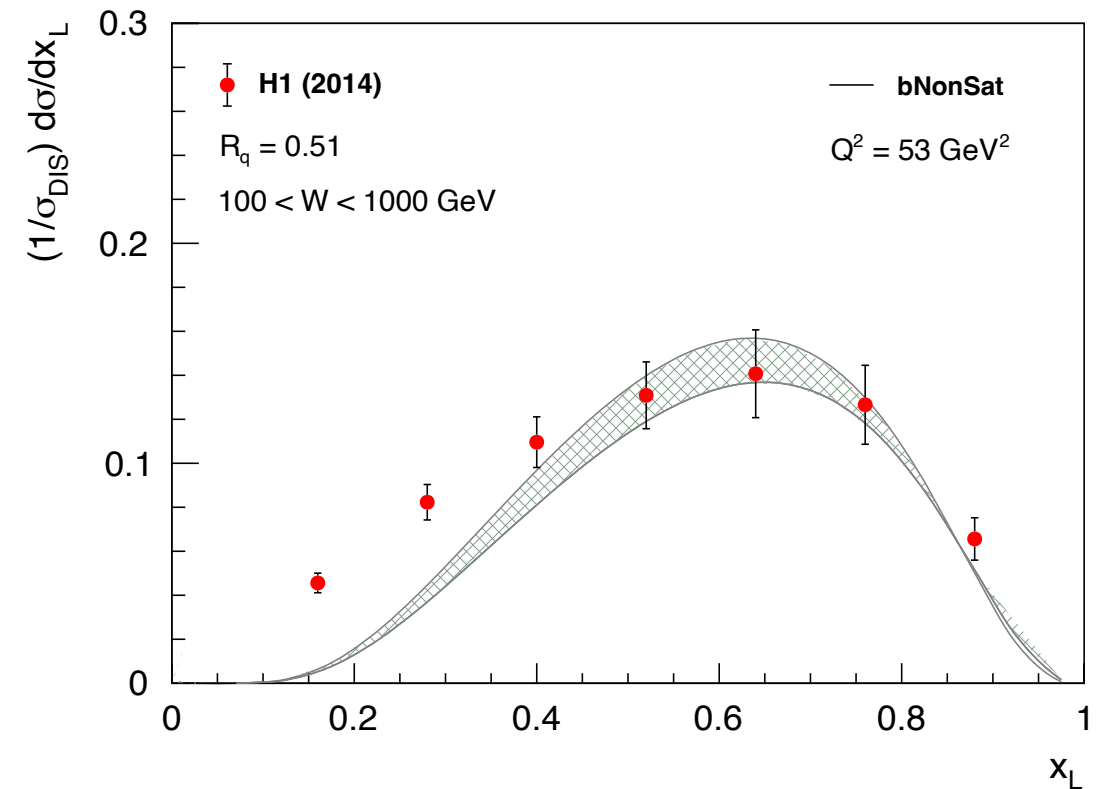
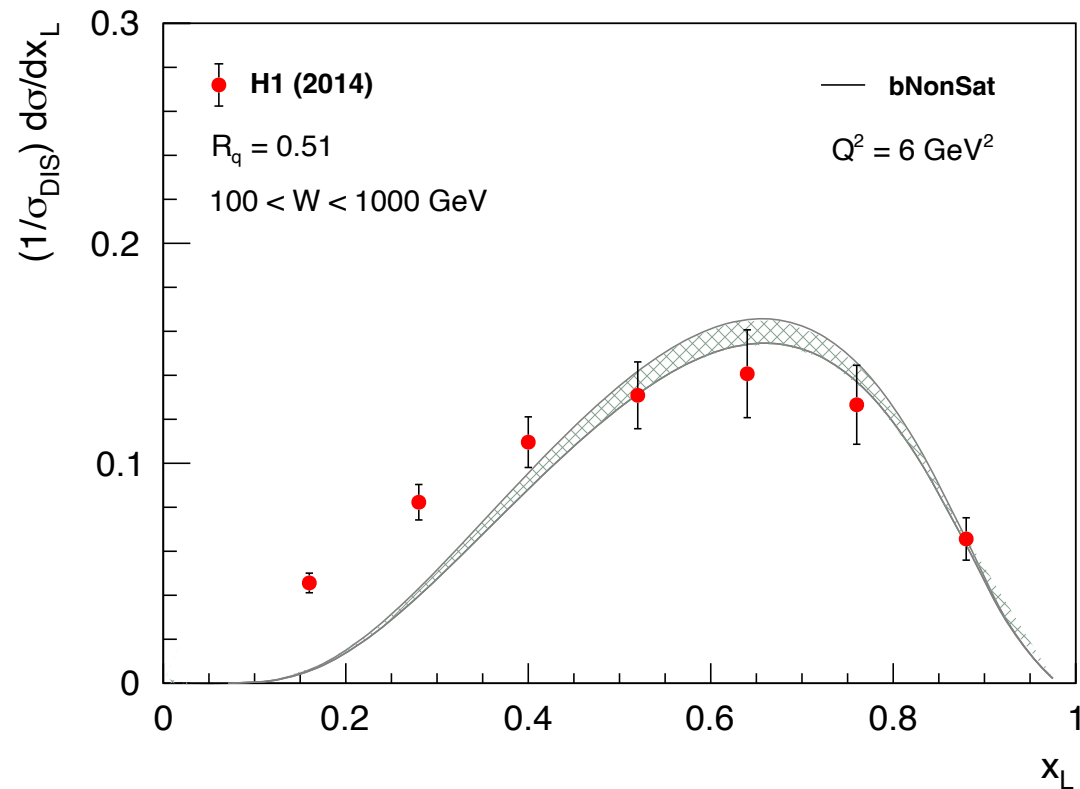
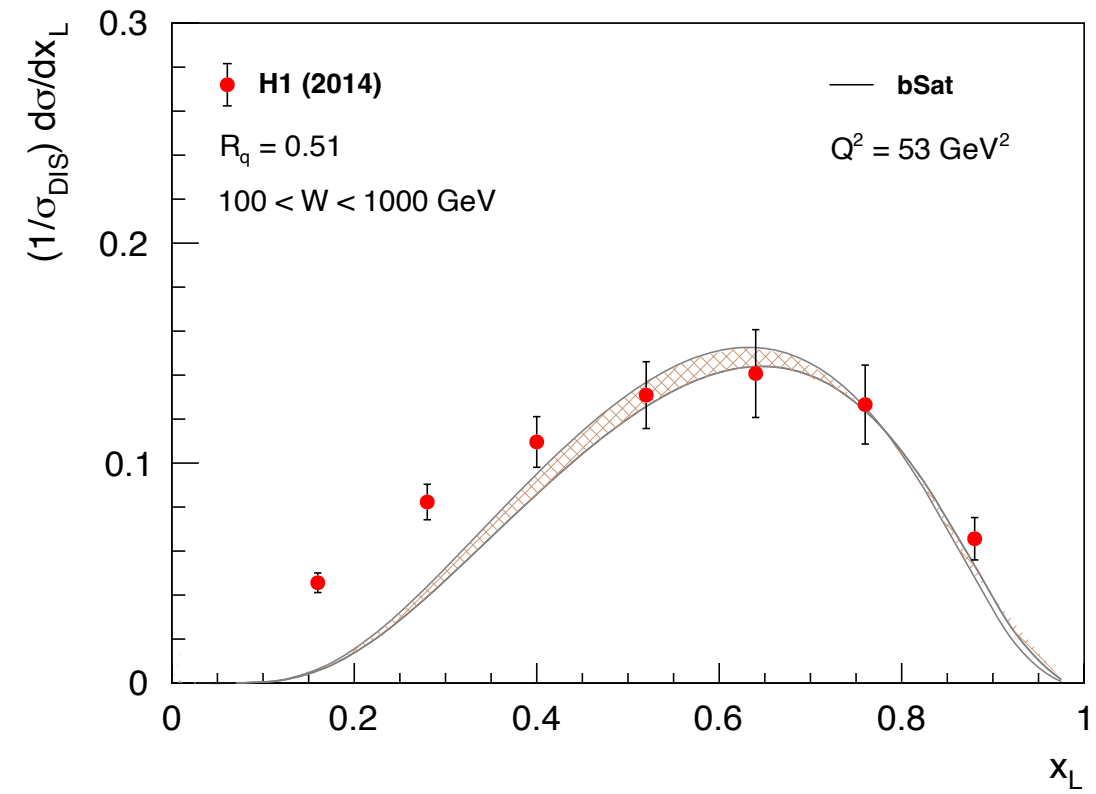
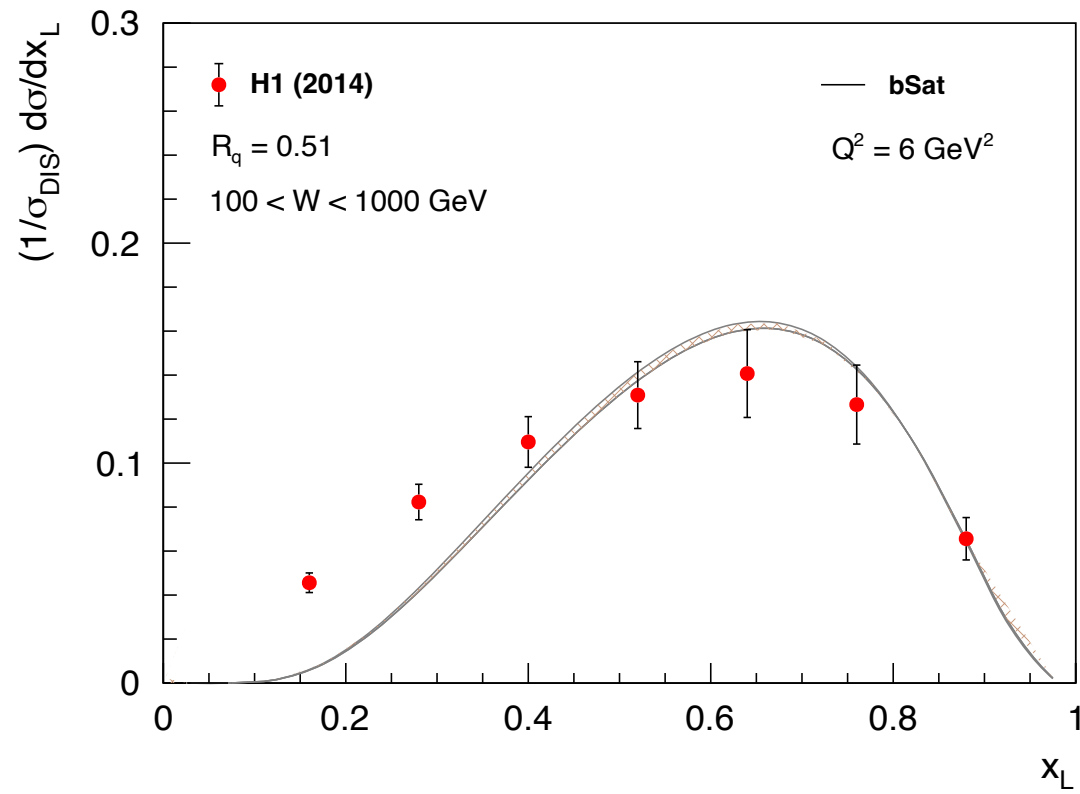


$$x_F \equiv x_L$$

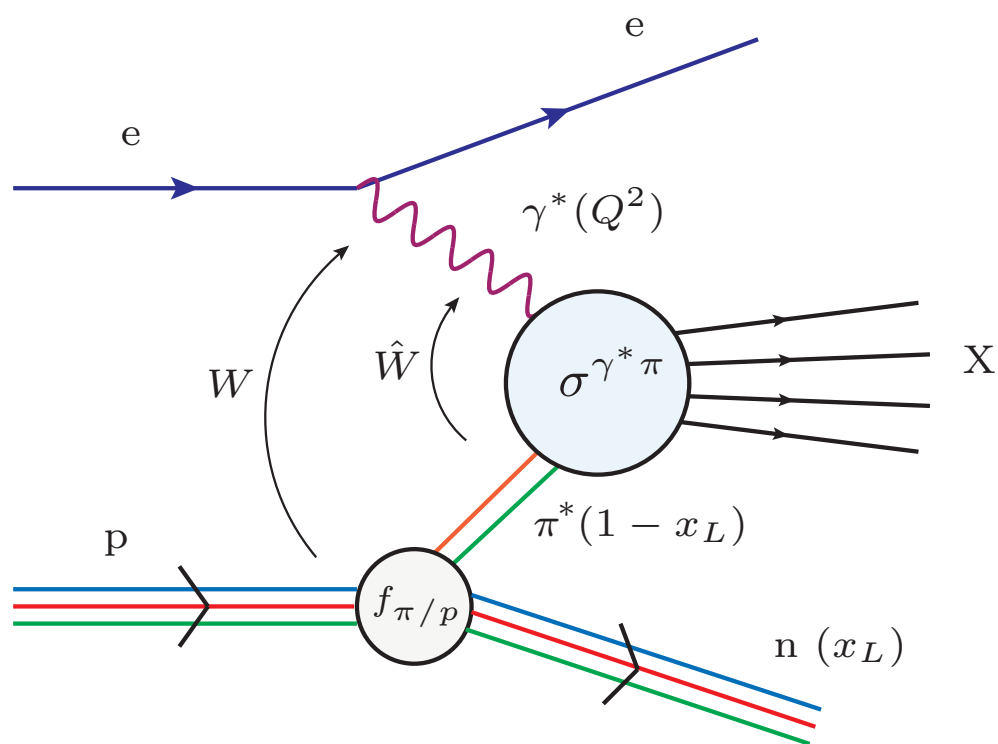
- ❖ Is this scaling related to saturation?
- ❖ Feynman scaling and its link with saturation
  - bCGC model [Carvalho, Gonçalves, Spiering, Navarra PLB 752 \(2016\) 76](#)

*“We demonstrate the recently released H1 leading neutron spectra can be described using the color dipole formalism and that these spectra could help us to observe more clearly gluon saturation effects in future ep colliders”*

# SCALING IN FEYNMAN-X SPECTRA



# INCLUSIVE CROSS SECTION WITH LEADING NEUTRONS



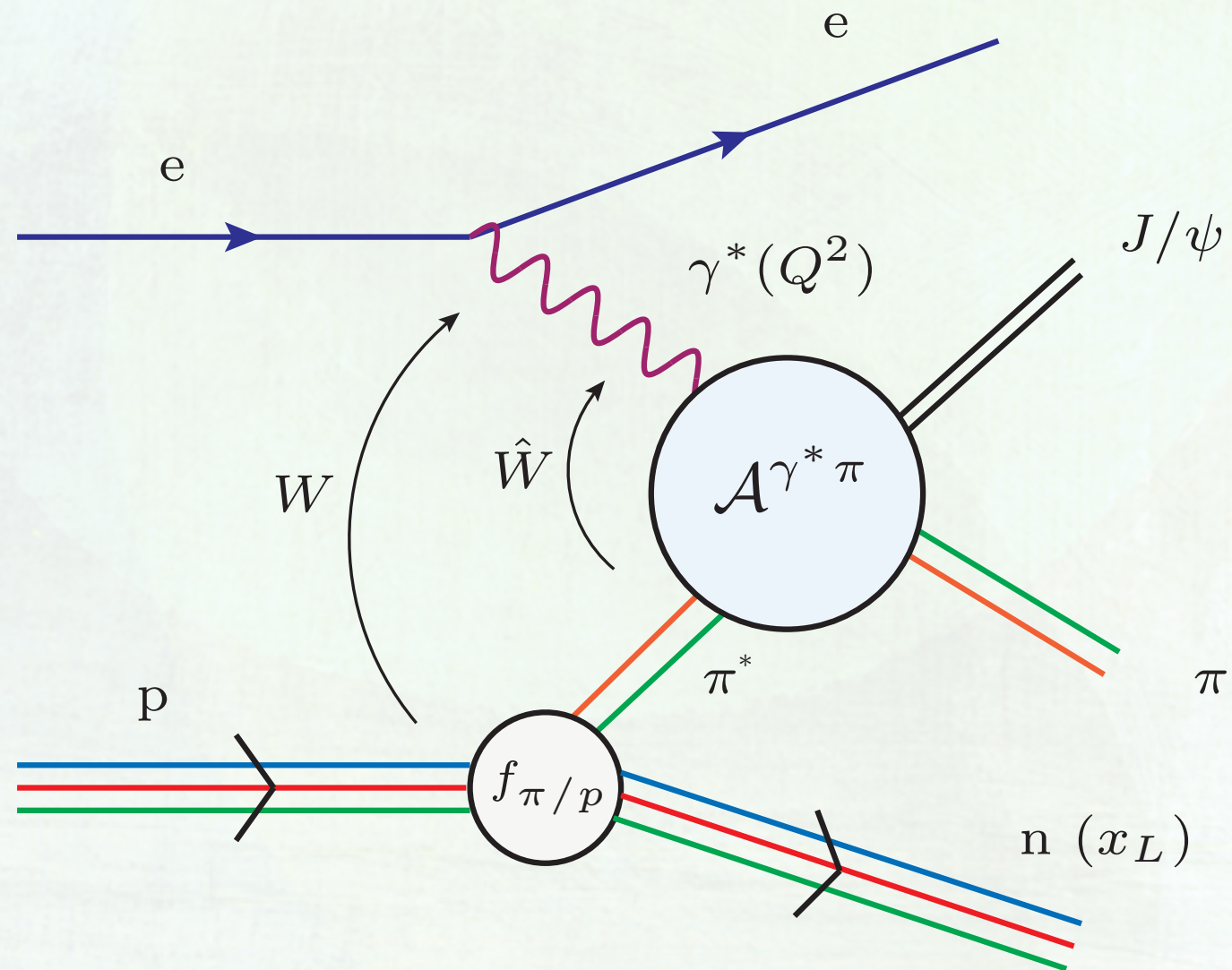
## WHAT WE HAVE LEARNT

- ❖ Dipole model phenomenology could successfully describe the leading neutron data (Feynman spectra and LN structure function)
- ❖ Constrain the gluon distribution of pions at small-x in the dipole framework
- ❖ Universality of the pion and proton structure at small-x upto normalisation
- ❖ The total  $\gamma^* \pi^*$  cross section shows geometric scaling behaviour
- ❖ LN data shows Feynman scaling and is unrelated to saturation
- ❖ No hints of saturation effects in LN data

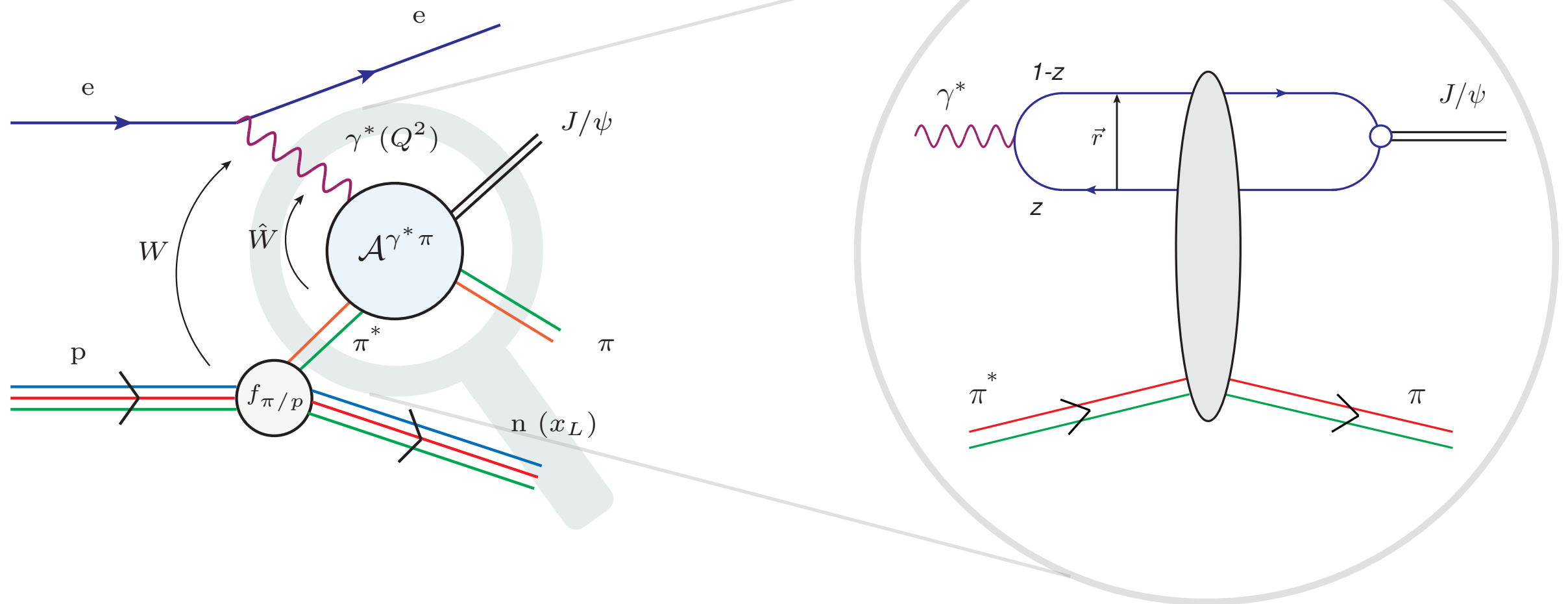


# EXCLUSIVE VM PRODUCTION WITH LEADING NEUTRONS

---

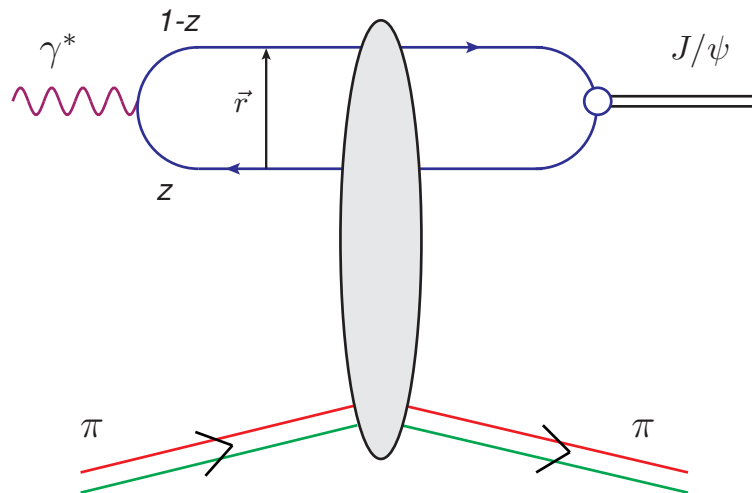


# EXCLUSIVE $J/\Psi$ PRODUCTION WITH LEADING NEUTRONS



- ❖ Exclusive measurement :  $e + p \rightarrow e' + J/\psi + \pi + n$
- ❖ Experimental signature : Rapidity gap between  $J/\psi$  and the pion
- ❖ More sensitive to non-linear effects and a good probe for transverse structure

# EXCLUSIVE $J/\Psi$ PRODUCTION WITH LEADING NEUTRONS



Various stages of exclusive  $J/\psi$  production in the dipole model:

1.  $\gamma^* \rightarrow q\bar{q}$  splitting ( $QED$ )
2. Dipole  $\rightarrow \pi^*$  scattering ( $model + QCD$ )
3. Dipole  $\rightarrow V.M$  ( $model$ )

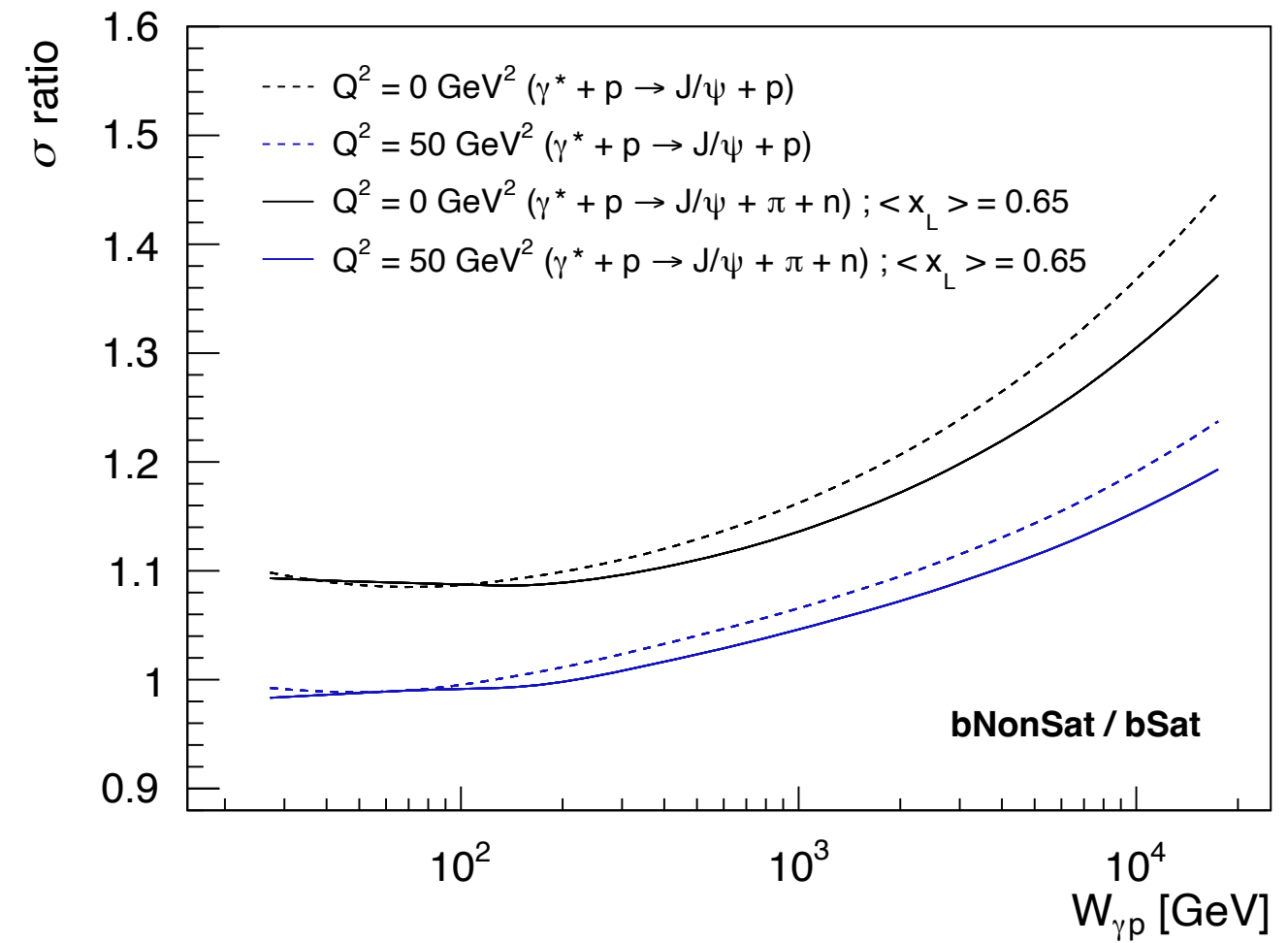
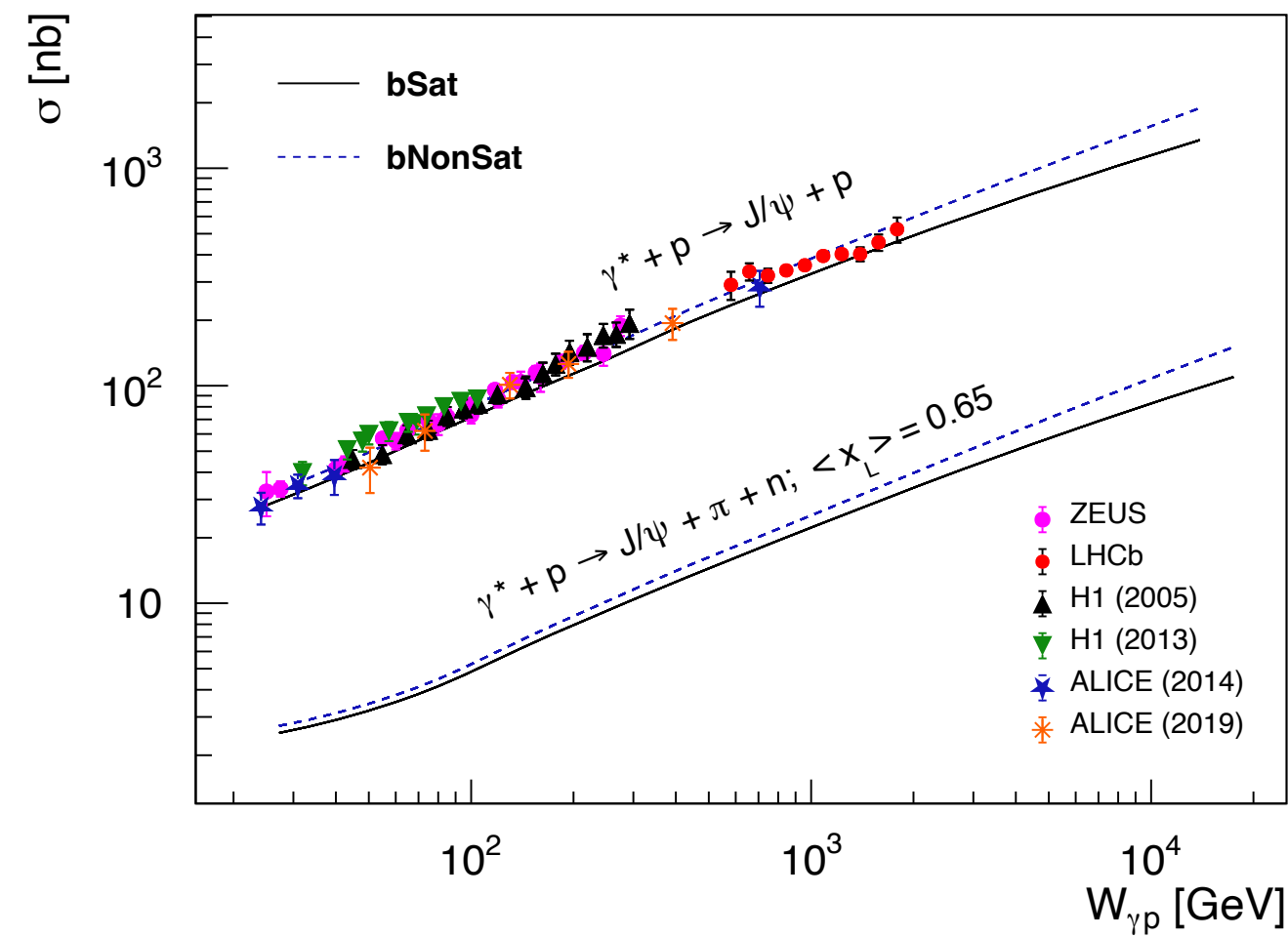
$$\mathcal{A}_{T,L}^{\gamma^* \pi^* \rightarrow J/\psi \pi}(\hat{x}, Q^2, \Delta) \sim \int d^2\mathbf{b} \int d^2\mathbf{r} \int dz (\Psi_V^* \Psi)_{L,T}(\mathbf{r}, z, Q^2) e^{i.\mathbf{b}.\Delta} \frac{d\sigma_{q\bar{q}}^{(\pi)}}{d^2\mathbf{b}}(\mathbf{b}, \mathbf{r}, \hat{x})$$

- ❖ Same dipole cross-section fitted from semi-inclusive data (bSat and bNonSat)
- ❖ Impact parameter is Fourier conjugate to momentum transfer, hence giving access to spatial structure of the target
- ❖ The differential cross section is

$$\frac{d\sigma_{T,L}^{\gamma^* p \rightarrow V p}}{dt} = \frac{1}{16\pi} \left| \mathcal{A}_{T,L}^{\gamma^* p \rightarrow V p} \right|^2 \sim [xg(x, Q^2)]^2$$

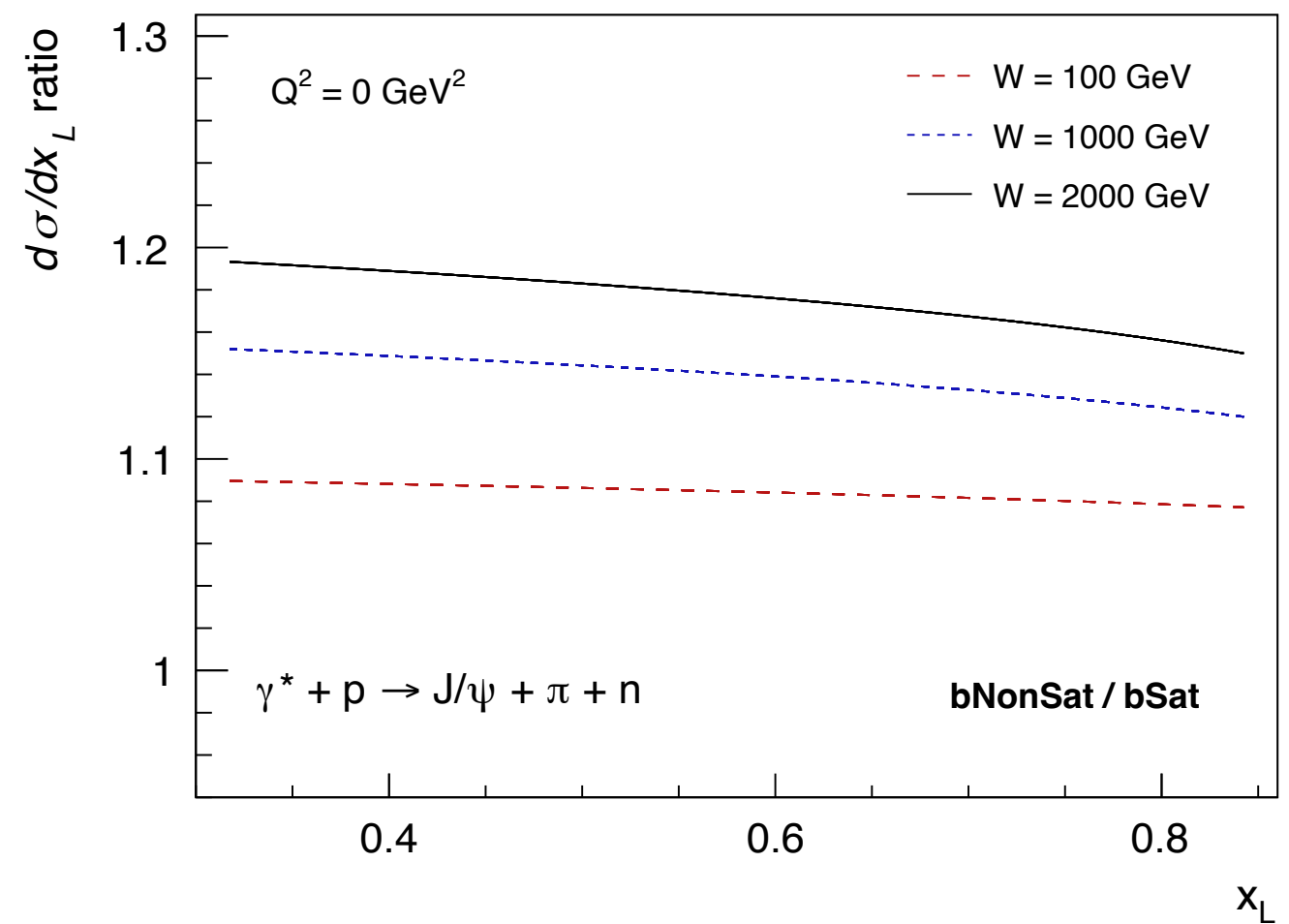
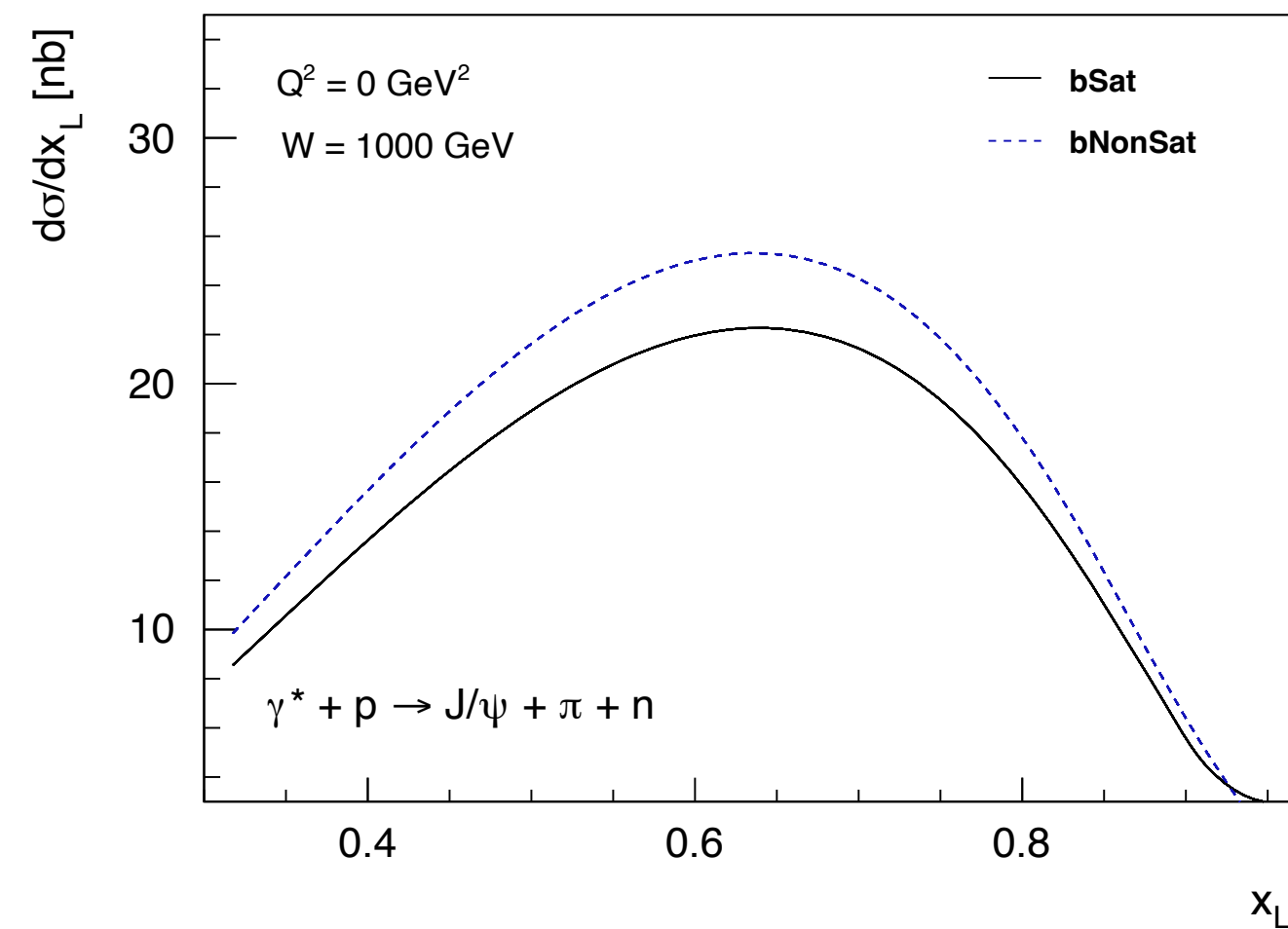


# ENERGY DEPENDENCE OF EXCLUSIVE $J/\Psi$ PRODUCTION

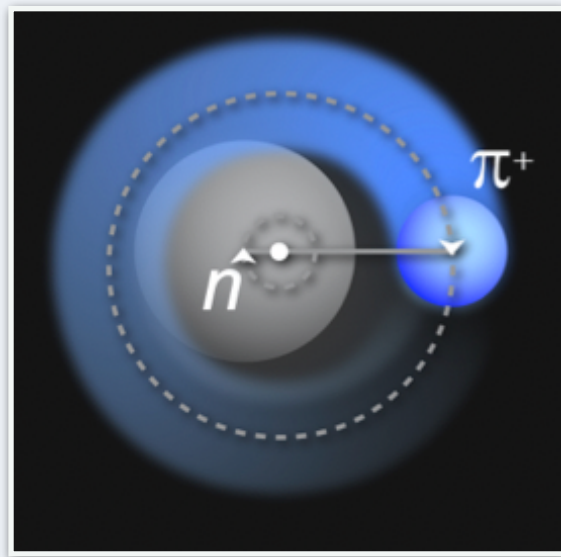
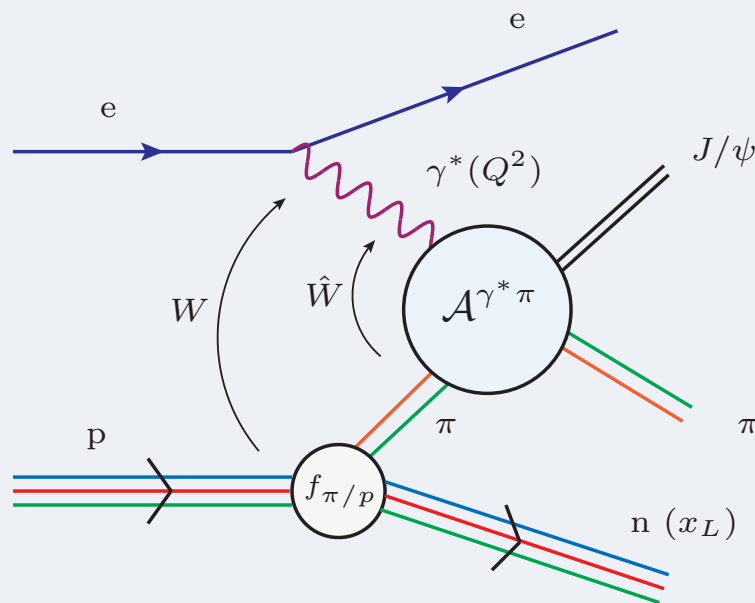




# EXCLUSIVE $J/\Psi$ PRODUCTION WITH LEADING NEUTRONS



# PROBING THE GLUON DISTRIBUTION



$$\sigma_{total} = \sigma_{yukawa} + \sigma_{fluctuations}$$

- ❖ The transverse profile of the virtual pion is,

$$T_{\pi^*}(b) = \int_{-\infty}^{\infty} dz \rho_{\pi^*}(b, z)$$

where the radial part of the virtual pion wave function is given by Yukawa theory:

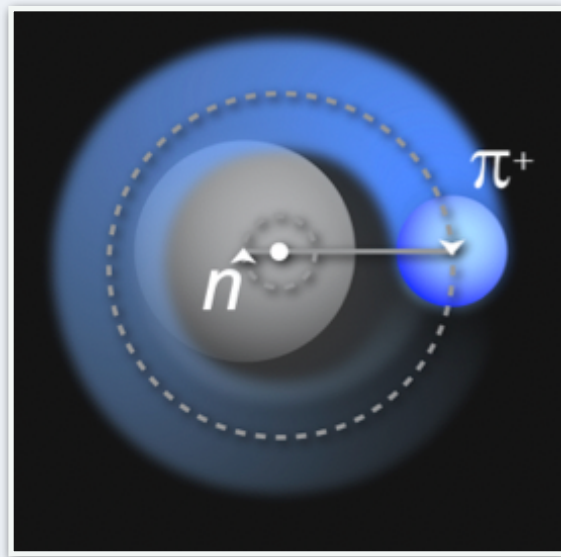
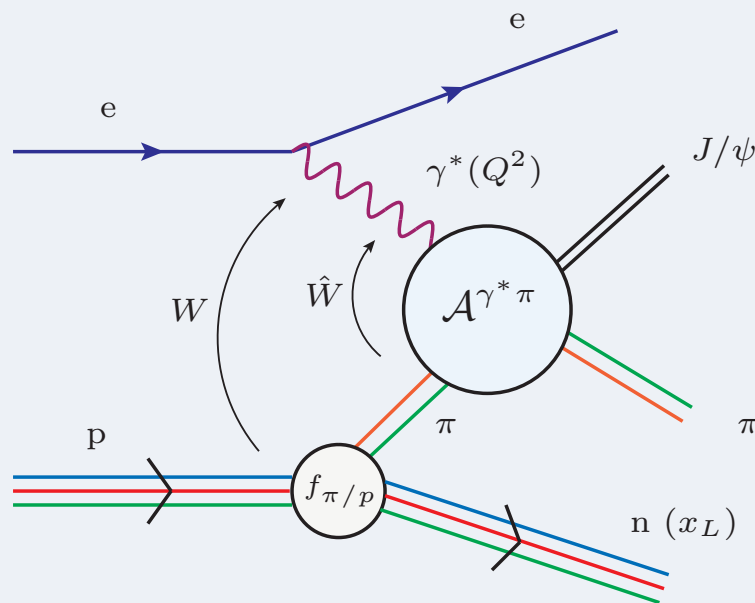
$$\rho_{\pi^*}(b, z) = \frac{m_{\pi}^2}{4\pi} \frac{e^{-m_{\pi} \sqrt{b^2 + z^2}}}{\sqrt{b^2 + z^2}}$$

- ❖ We assume that the real pion, as for the proton, is described by a Gaussian profile:

$$T_{\pi}(b) = \frac{1}{2\pi B_{\pi}} e^{-\frac{b^2}{2B_{\pi}}}$$

- ❖ At small  $|t'|$ , the dipole cannot resolve the pion and interacts with the whole cloud and on increasing the resolution (*increasing*  $|t'|$ ) the dipole interacts with the pion
- ❖ The transverse position of the pion inside the virtual pion cloud fluctuates event by event

# PROBING THE GLUON DISTRIBUTION



$$\sigma_{total} = \sigma_{yukawa} + \sigma_{fluctuations}$$

❖ The thickness function of pion:

$$T_{\pi}(b) = \frac{1}{2\pi B_{\pi}} e^{-\frac{b^2}{2B_{\pi}}}, \quad B_{\pi} \text{ is the transverse width of the pion}$$

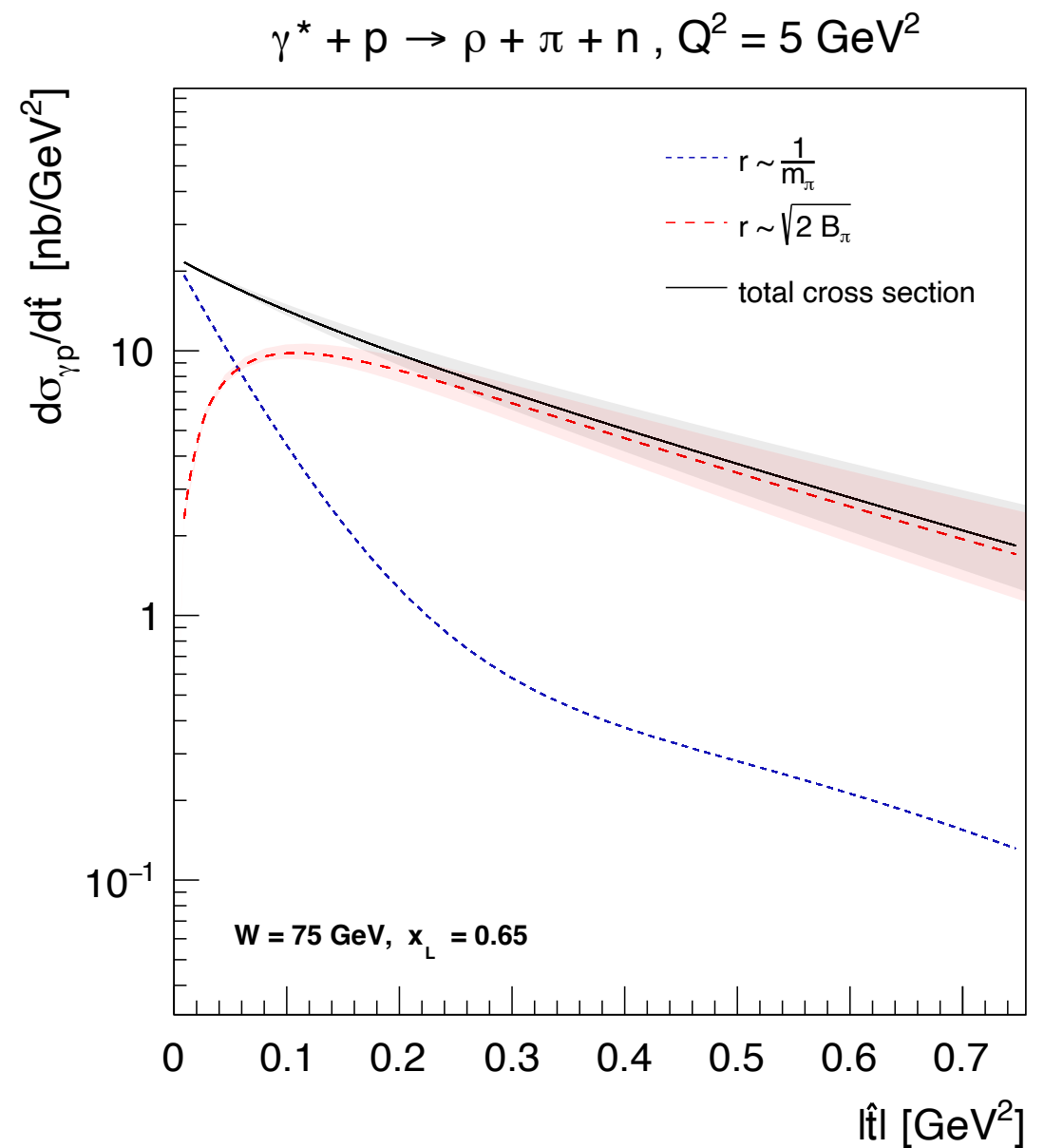
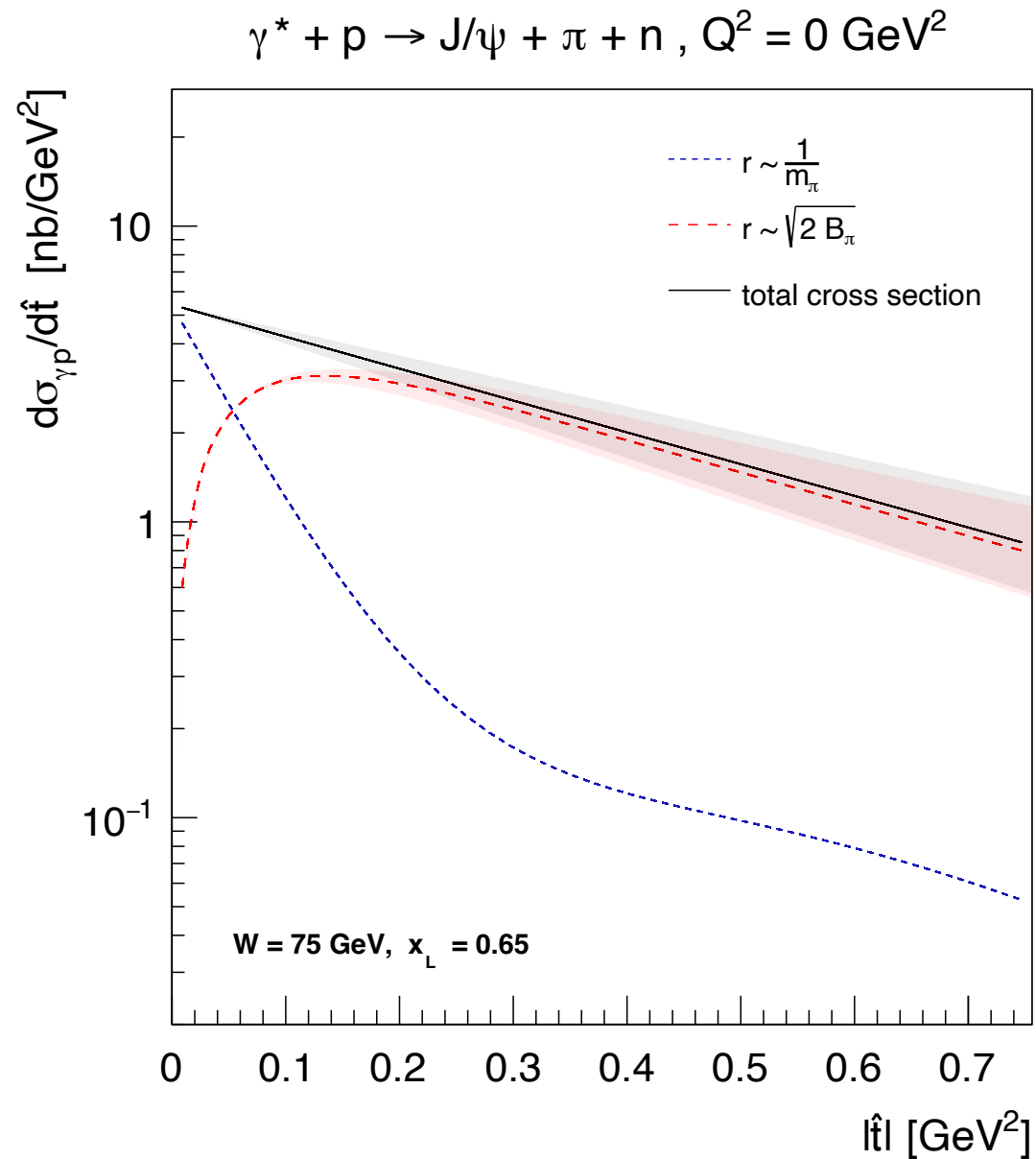
❖ No experimental data on  $l_t$  dependence which can restrict this parameter

- Assume that the gluon to charge radius is same in pions and protons:  $B_{\pi} = r_{\pi}^2 / r_p^2 B_p = (0.657/0.840)^2 \cdot 4^{-2} \approx 2.44 \text{ GeV}^{-2}$
- Pion gluon radius from the Belle measurements at KEKB in hadron-pair production  $\gamma^* \gamma \rightarrow \pi^0 \pi^0$  which suggests  $B_{\pi} \approx 1.33 - 1.96 \text{ GeV}^{-2}$  [Kumano et al PRD 97 \(2018\), 014020](#)
- H1 measured the  $l_t$  spectrum for exclusive  $\rho$  photo-production with leading neutrons in  $ep$  scattering, as this process lacks a hard scale we are not able to make a direct comparison, but this spectrum suggests  $B_{\pi} \approx 2.3 \text{ GeV}^{-2}$  [HI EPJC 76 \(2016\), 41](#)

❖ We therefore present our results with bands for

$$B_{\pi} = 2 \pm 0.5 \text{ GeV}^{-2}$$

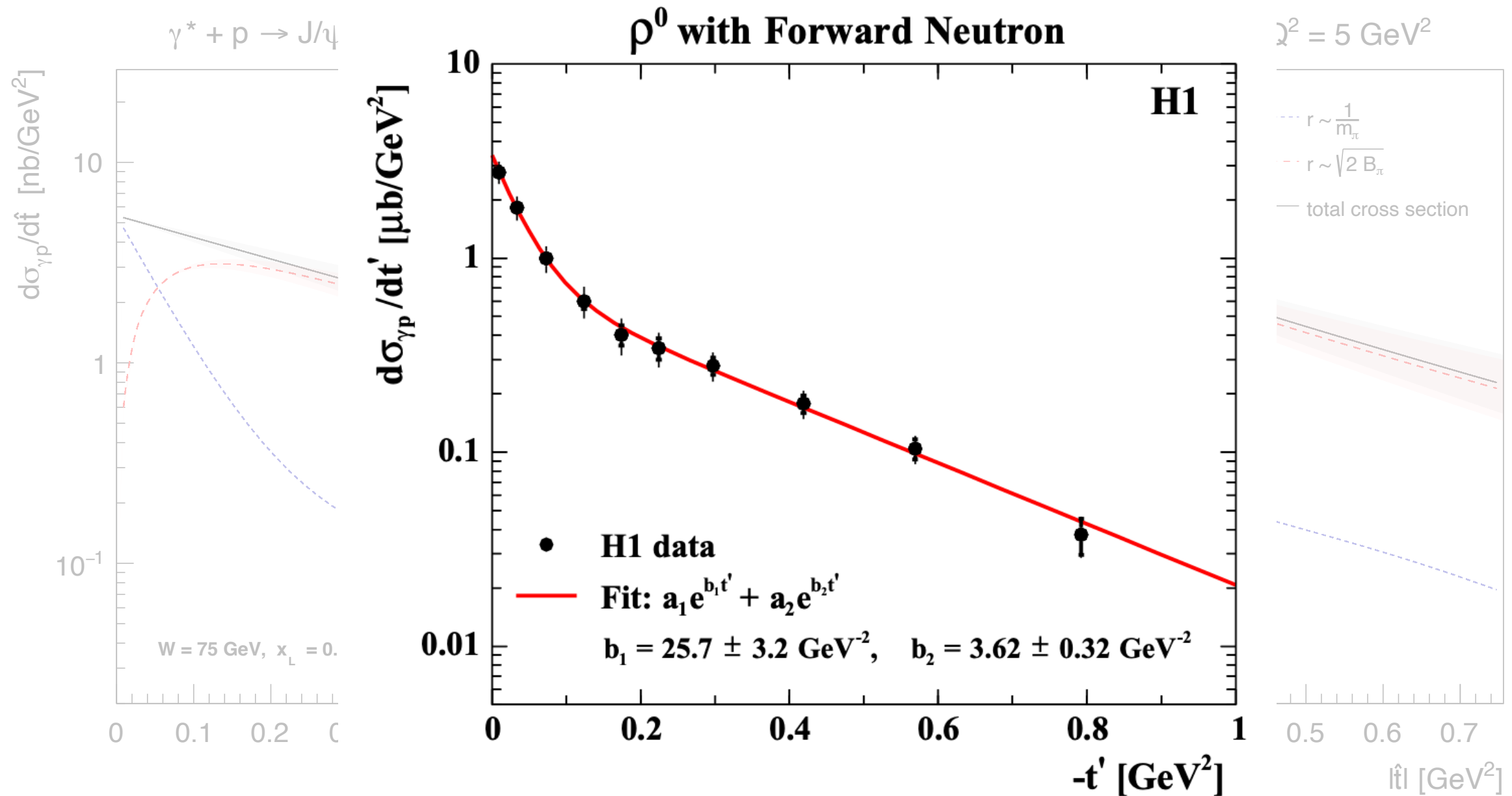
# PROBING THE GLUON DISTRIBUTION



- ❖ The cross section have two slopes due to interaction with different size scales at low  $|t'|$  and moderate  $|t'|$
- ❖ H1 data on exclusive  $\rho$  photo production with leading neutrons exhibits these two slopes in the differential distribution

# PROBING THE GLUON DISTRIBUTION

H1 EPJC 76 (2016), 41



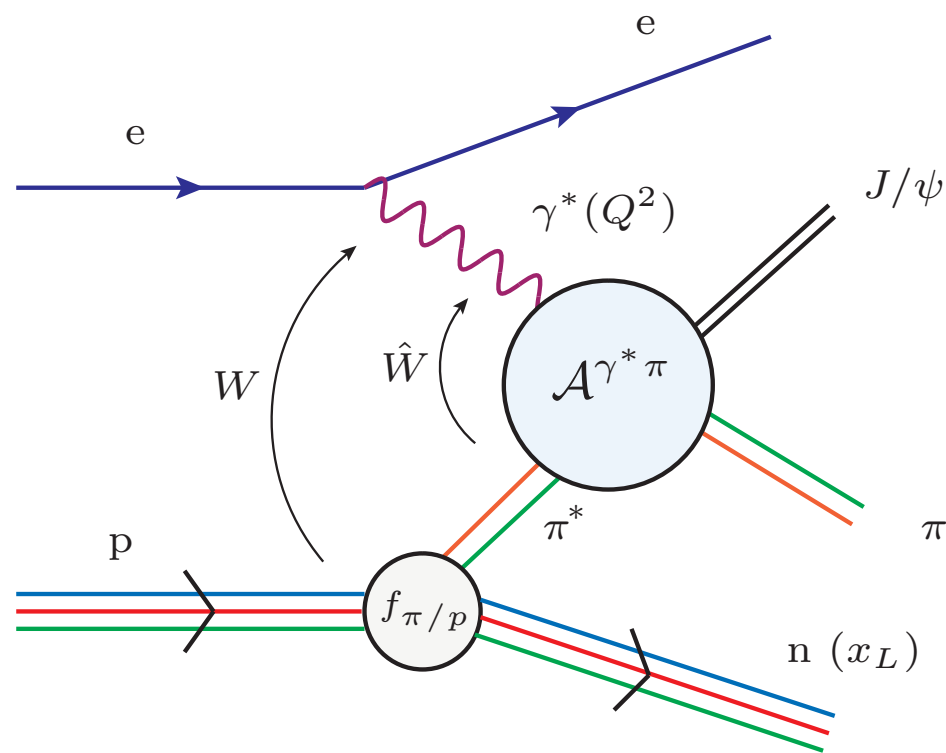
- ❖ The cross section have two slopes due to interaction with different size scales at low  $|t'|$  and moderate  $|t'|$
- ❖ H1 data on exclusive  $\rho$  photo production with leading neutrons exhibits these two slopes in the differential distribution



# EXCLUSIVE MEASUREMENTS WITH LEADING NEUTRONS

---

## WHAT WE HAVE LEARNT



- ❖ Dipole model provides a unified framework to study inclusive and exclusive events
- ❖ The total exclusive  $J/\psi$  cross section is sensitive to saturation at high energies
- ❖ Feynman spectra of leading neutrons could be used to look for saturation effects at high energies
- ❖ Usual exclusive events with proton are more sensitive to saturation
- ❖ Probe for transverse gluon distribution of pions and a first prediction of t-spectrum of gluon distribution
- ❖ Direct evidence for proton fluctuation into pion and neutron

# SUMMARY AND OUTLOOK

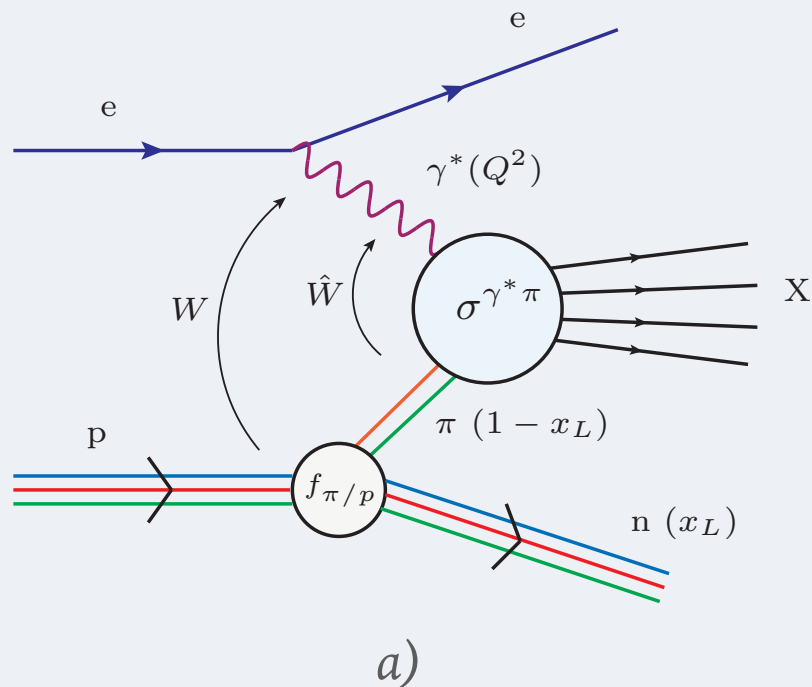
---

- ❖ Investigated virtual photon scattering with the pion cloud of proton in  $ep$  scattering using dipole model
  - Semi-inclusive measurement:
    - Probe the longitudinal structure of pions
    - Universal structure of the pion and proton upto normalisation
    - Data shows Geometric and Feynman scaling behaviour
    - Both the saturated and non-saturated model describes the data
  - Exclusive measurement:
    - Sensitive to non-linear or saturation effects but less so than that of protons
    - Probe for gluon radius of the pion
    - Direct evidence of a proton fluctuation into pion and neutron
- ❖ Future experiments such as EIC and LHeC can measure the exclusively produces vector meson production in  $ep$  scattering with leading neutron events
- ❖ Measurement of photo-nuclear cross sections in UPC's at LHC and RHIC are good tests for our models and saturation physics.

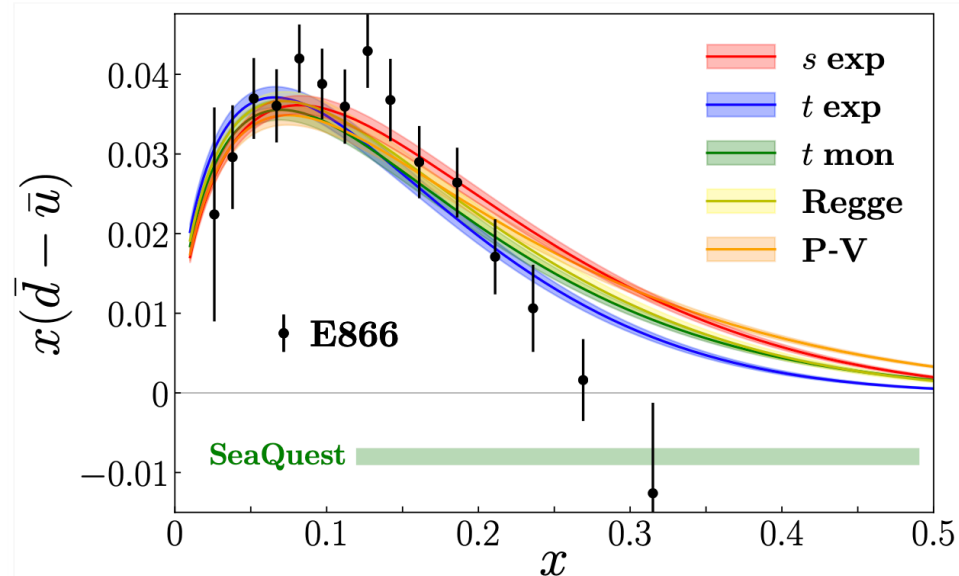
THANK YOU

# BACKUP

# FLAVOUR ASYMMETRY AND PION CLOUD



- ❖ Access to the structure function of “pion” via Sullivan process [J.D. Sullivan PRD 5 \(1972\), 1732](#)
- ❖ How does gluon density behave in the pion? Is there any universal behaviour at small-x ?
- ❖ How are gluons distributed inside pions? What is the gluon radius of pion?
- ❖ Sensitivity to the saturation effects
- ❖ Feynman scaling and its link with saturation
  - bCGC model [Carvalho, Gonçalves, Spiering, Navarra PLB 752 \(2016\) 76](#)
- ❖ Evidence of the pion cloud of the proton



[Barry et al PRL 121, 152001](#)

- Pions are main building blocks of nuclear matter
- Pion cloud models explain the light-quark asymmetry in the nucleon sea
- Pions are the Yukawa particles of the nuclear force (no evidence of excess)

# PION FLUX MODELS

Carvalho, Gonçalves, Spiering, Navarra PLB 752 (2016) 76

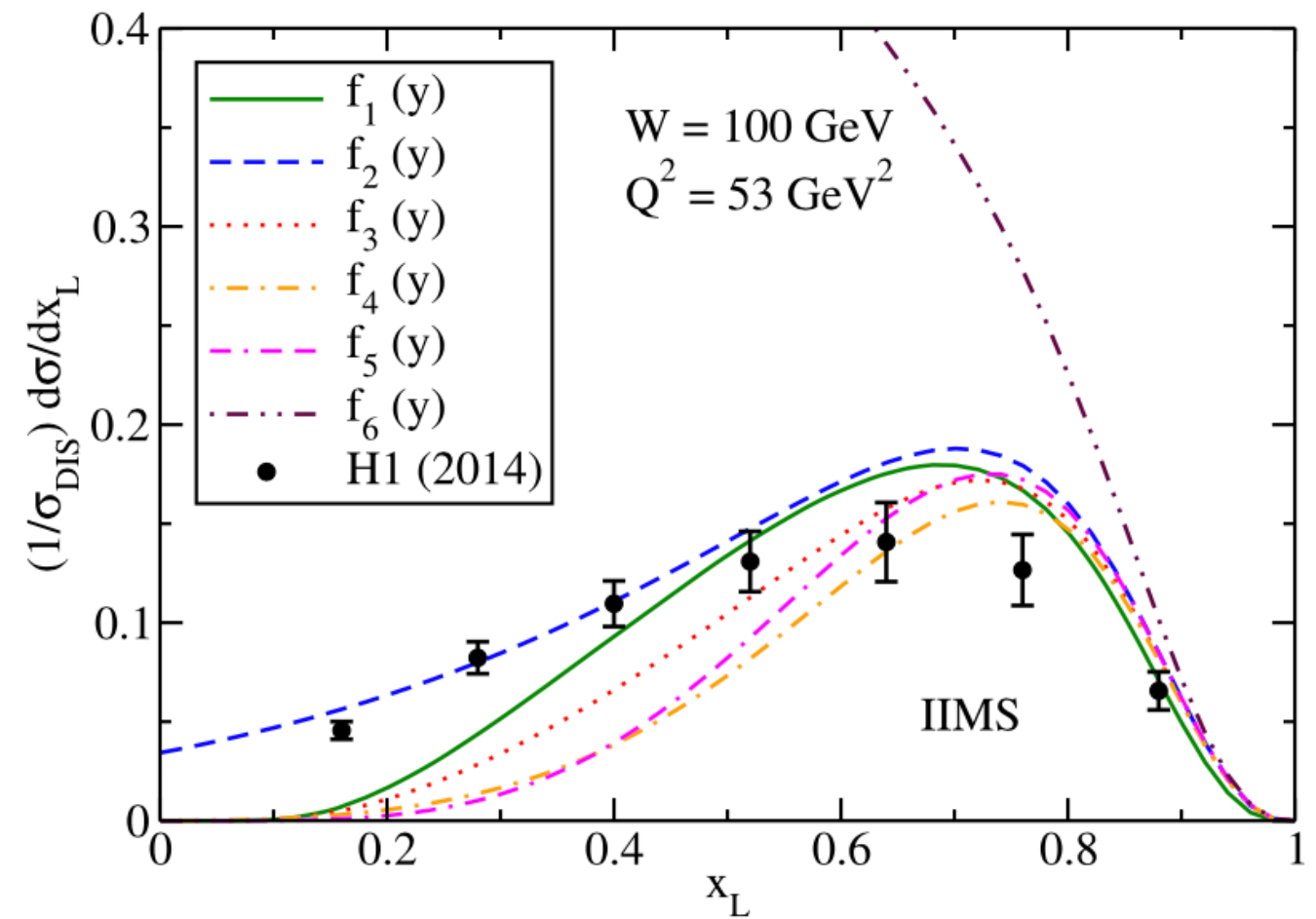
$$F_1(x_L, t) = \exp \left[ R^2 \frac{(t - m_\pi^2)}{(1 - x_L)} \right], \quad \alpha(t) = 0$$

$$F_2(x_L, t) = 1, \quad \alpha(t) = \alpha(t)_\pi$$

$$F_3(x_L, t) = \exp \left[ b(t - m_\pi^2) \right], \quad \alpha(t) = \alpha(t)_\pi$$

$$F_4(x_L, t) = \frac{\Lambda_m^2 - m_\pi^2}{\Lambda_m^2 - t}, \quad \alpha(t) = 0$$

$$F_5(x_L, t) = \left[ \frac{\Lambda_d^2 - m_\pi^2}{\Lambda_d^2 - t} \right]^2, \quad \alpha(t) = 0$$

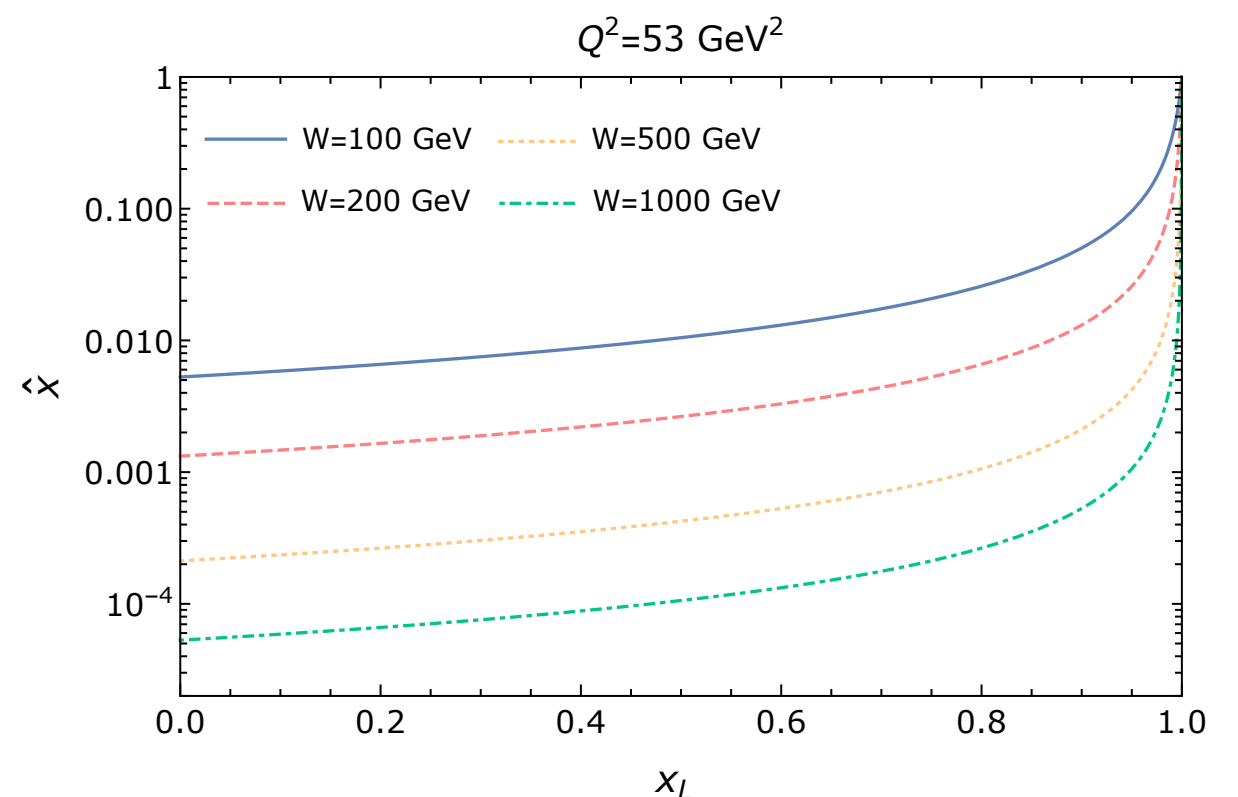
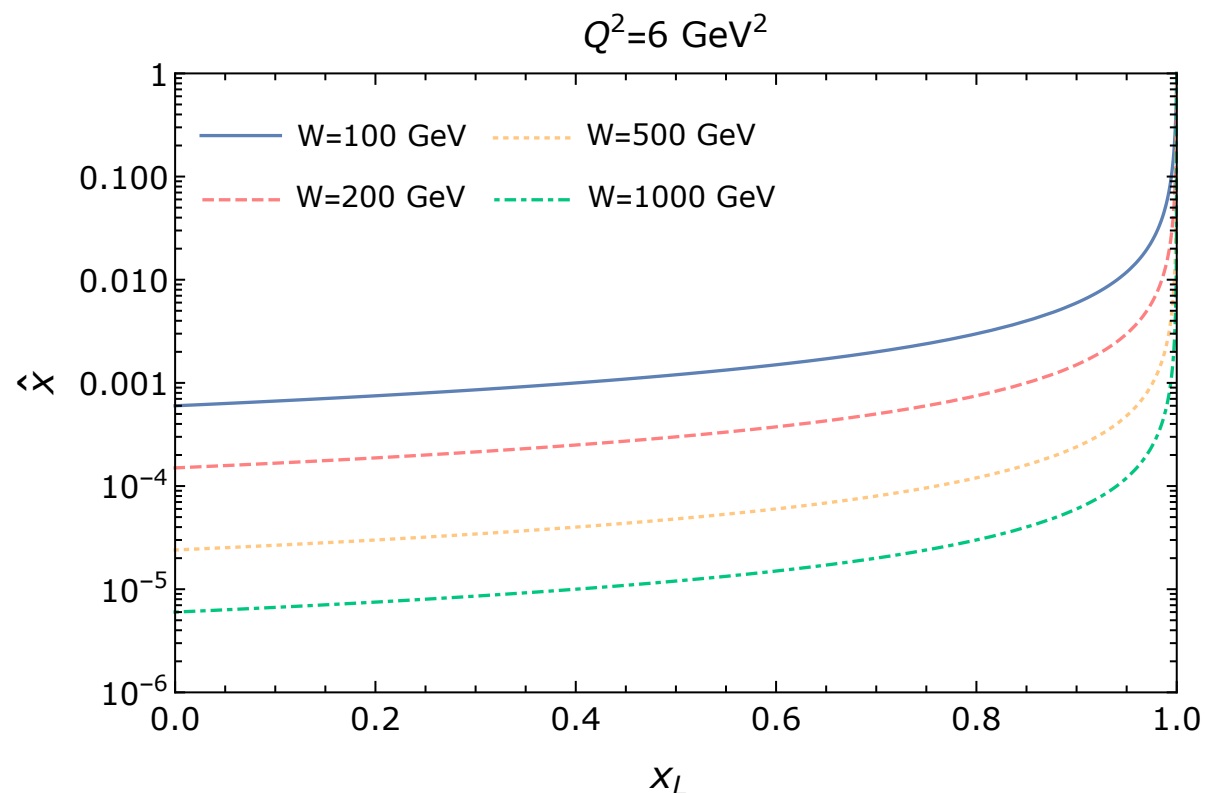


(a)

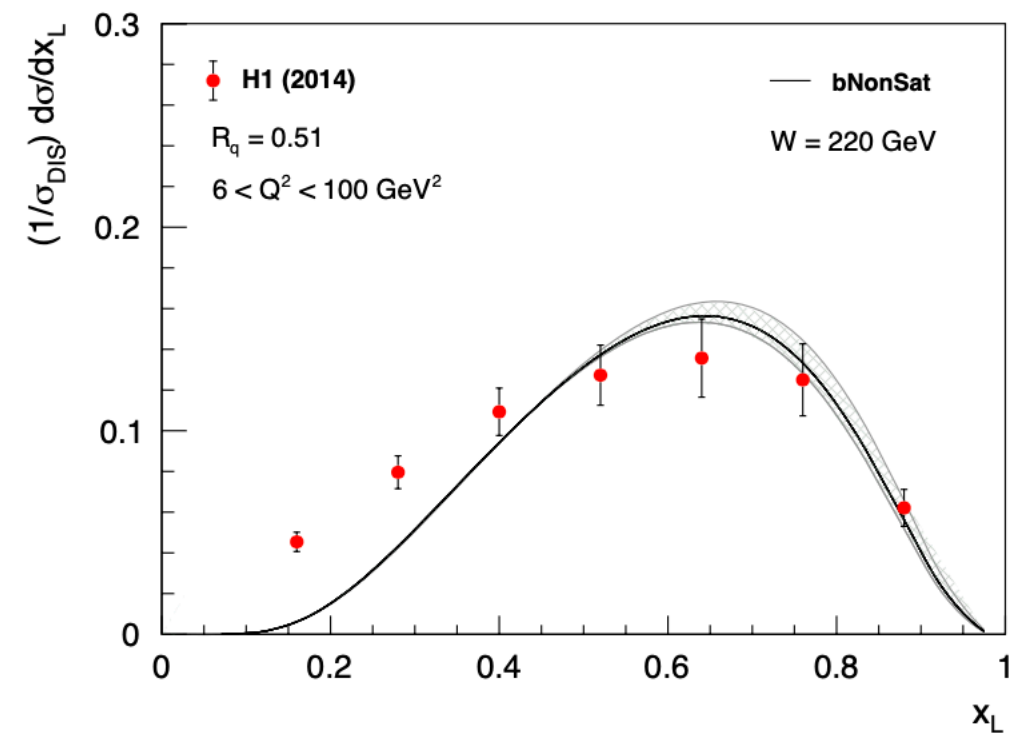
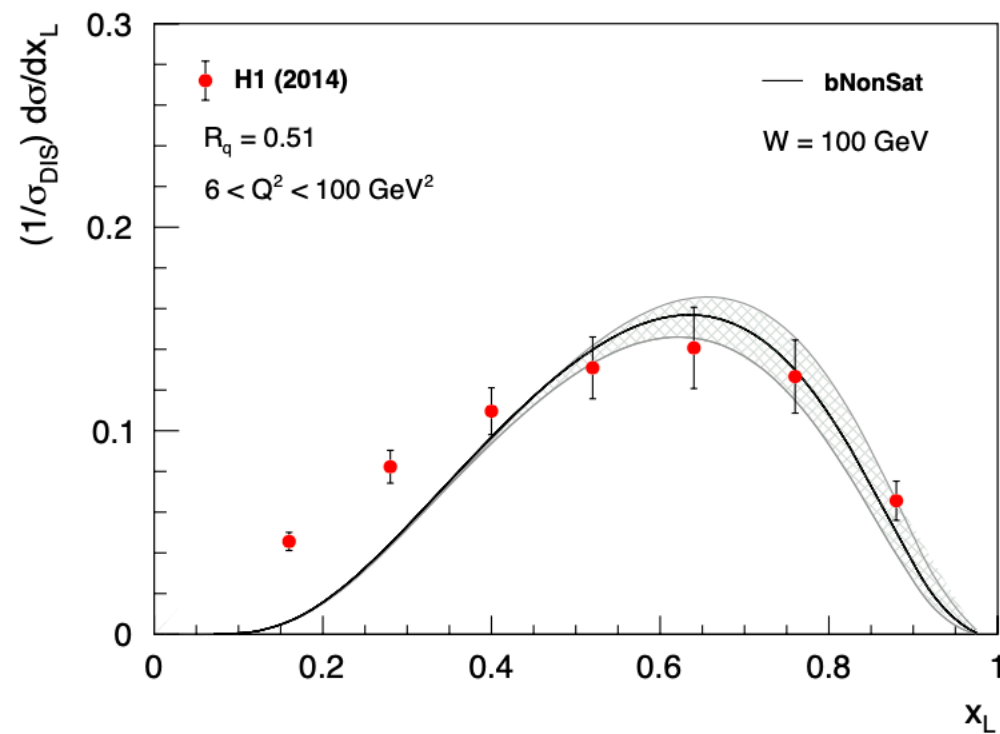
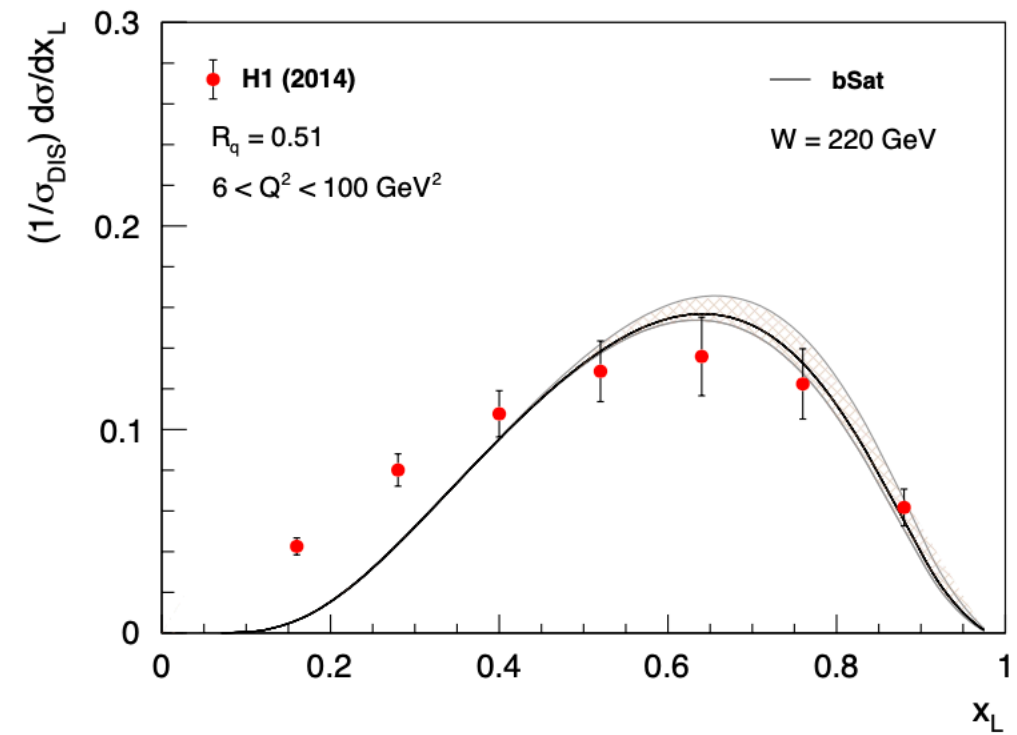
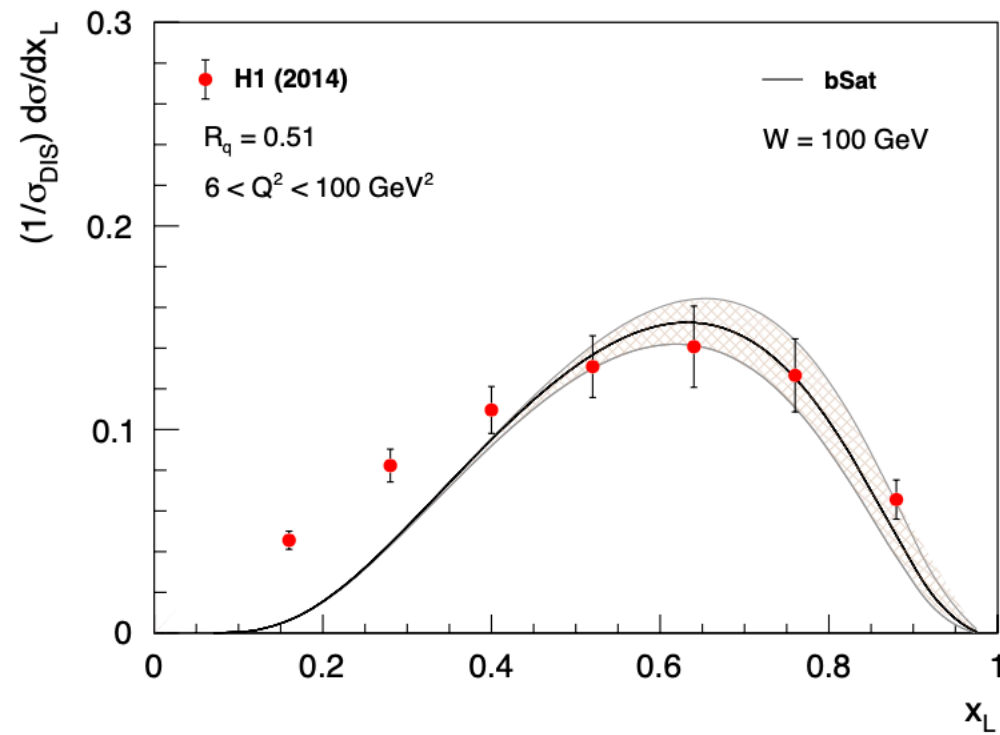


# LN AS A PROBE FOR SMALL-X PHYSICS

- ❖ The x value probed in such a process is  $\hat{x} = \frac{Q^2 + m_f^2}{\hat{W}^2 + Q^2} = \frac{Q^2 + m_f^2}{(1 - x_L)W^2 + Q^2}$
- ❖ LN production is low x physics
- ❖ In principle, we could use the color dipole framework to investigate the pion properties at small-x
- ❖ Use the dipole model to calculate the pion structure function  $F_2^\pi$  and the leading neutron structure function  $F_2^{LN}$  to compare with the HERA Data



# $Q^2$ SCALING IN FEYNMAN-X SPECTRA



# MASS RADIUS OF PION USING GENERALISED DISTRIBUTION AMPLITUDES

Kumano, Song, Teryaev PRD 97 (2018), 014020

## Hadron tomography by generalized distribution amplitudes in pion-pair production process $\gamma^*\gamma \rightarrow \pi^0\pi^0$ and gravitational form factors for pion

S. Kumano,<sup>1,2,3</sup> Qin-Tao Song,<sup>1,3</sup> and O. V. Teryaev<sup>1,4</sup>

<sup>1</sup>KEK Theory Center, Institute of Particle and Nuclear Studies,  
High Energy Accelerator Research Organization (KEK),  
1-1, Oho, Tsukuba, Ibaraki, 305-0801, Japan

<sup>2</sup>J-PARC Branch, KEK Theory Center, Institute of Particle and Nuclear Studies, KEK,  
and Theory Group, Particle and Nuclear Physics Division, J-PARC Center,  
203-1, Shirakata, Tokai, Ibaraki, 319-1106, Japan

<sup>3</sup>Department of Particle and Nuclear Physics,  
Graduate University for Advanced Studies (SOKENDAI),  
1-1, Oho, Tsukuba, Ibaraki, 305-0801, Japan

<sup>4</sup>Bogoliubov Laboratory of Theoretical Physics,  
Joint Institute for Nuclear Research, 141980 Dubna, Russia

(Dated: January 10, 2019)

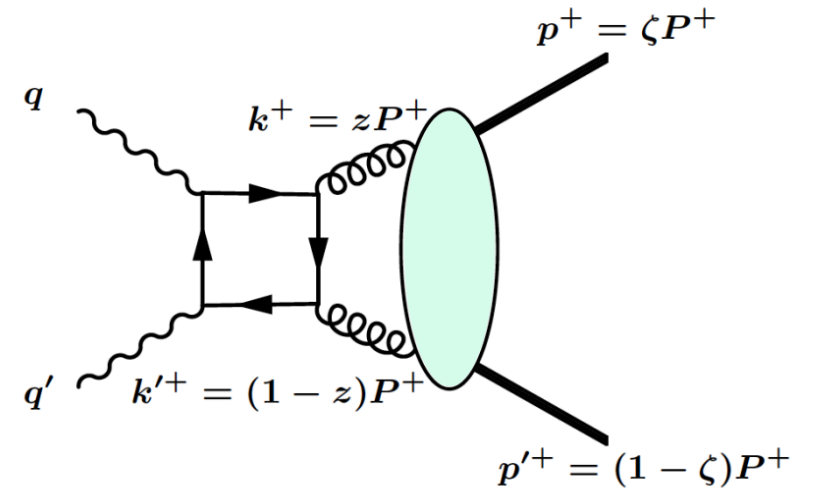


FIG. 4. Contribution to the two-photon cross section from the gluon GDA.

Hadron tomography can be investigated by three-dimensional structure functions such as generalized parton distributions (GPDs), transverse-momentum-dependent parton distributions, and generalized distribution amplitudes (GDAs). Here, we extract the GDAs, which are  $s$ - $t$  crossed quantities of the GPDs, from cross-section measurements of hadron-pair production process  $\gamma^*\gamma \rightarrow \pi^0\pi^0$  at KEKB. This work is the first attempt to obtain the GDAs from the actual experimental data. The GDAs are expressed by a number of parameters and they are determined from the data of  $\gamma^*\gamma \rightarrow \pi^0\pi^0$  by including intermediate scalar- and tensor-meson contributions to the cross section. Our results indicate that the dependence of parton-momentum fraction  $z$  in the GDAs is close to the

$$\sqrt{\langle r^2 \rangle_{\text{mass}}} = 0.32 \sim 0.39 \text{ fm},$$

$$\sqrt{\langle r^2 \rangle_{\text{mech}}} = 0.82 \sim 0.88 \text{ fm}.$$

# GOOD-WALKER FORMALISM

- Coherent cross-section probes **average  $\mathbf{b}$  dependence**  $\langle N(\mathbf{b}, \mathbf{r}, \mathbf{x}) \rangle_\Omega$  of dipole amplitude which provides the information about target geometry

$$\frac{d\sigma_{T,L}^{\gamma^* p \rightarrow V p}}{dt} = \frac{1}{16\pi} \left| \langle \mathcal{A}_{T,L}^{\gamma^* p \rightarrow V p} \rangle_\Omega \right|^2$$

- Incoherent cross-section** : target dissociates ( $\mathbf{f} \neq \mathbf{i}$ ) Good, Walker 1960, Miettinen, Pumplin 1978

$$\begin{aligned} \sigma_{incoherent} &\sim \sum_{\mathbf{f} \neq \mathbf{i}} \left| \langle \mathbf{f} | \mathcal{A} | \mathbf{i} \rangle \right|^2 \\ &= \sum_{\mathbf{f}} \langle \mathbf{i} | \mathcal{A}^\dagger | \mathbf{f} \rangle \langle \mathbf{f} | \mathcal{A} | \mathbf{i} \rangle - \langle \mathbf{i} | \mathcal{A} | \mathbf{i} \rangle^\dagger \langle \mathbf{i} | \mathcal{A} | \mathbf{i} \rangle \\ &= \langle |\mathcal{A}|^2 \rangle_\Omega - \left| \langle \mathcal{A} \rangle_\Omega \right|^2 \end{aligned}$$

$$\frac{d\sigma_{total}}{dt} = \frac{1}{16\pi} \langle |\mathcal{A}|^2 \rangle_\Omega$$

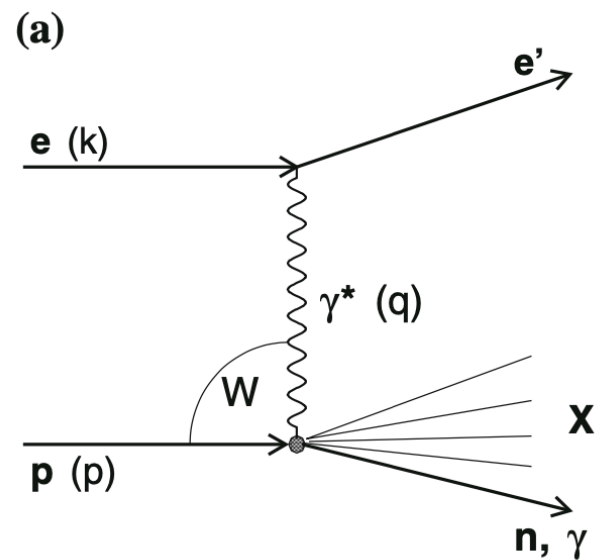
$$\frac{d\sigma_{coherent}}{dt} = \frac{1}{16\pi} \left| \langle \mathcal{A} \rangle_\Omega \right|^2$$

- Incoherent cross-section is the **variance** of amplitude which controls the amount of event-by-event fluctuations in target configurations

# FEYNMAN-X SPECTRA AT SMALL -XL

HI EPJC 74 (2014), 2915

Standard fragmentation (DJANGO)



One-pion approximation (RAPGAP)

